From chaos to stability: the development of an alternating bar-channel estuary

Utrecht University, Department of Physical Geography
Utrecht, The Netherlands

Utrecht University

MSc thesis
J.M. de Lange
Student number: 4122968
May 2018 – October 2019

Master: Earth Surface and Water
Supervisors: Dr M.G. Kleinhans
MSc J.R.F.W Leuven

Cover clarification:

“Your happiness is at the intersection of your passions and learning from great people.”
– Scott Weiss

The photograph on the cover of this thesis was taken by Jacco Quist during the Tacx Pro Classic, 2018. At that moment, the peloton made its way over the Kattendijksedijk. This dike separates the former estuary Western Scheldt and my home town. Racing there (white shoe and yellow helmet on the far right), supported by my family and friends, is where my passions intersected.

Contents

Abstract

Estuaries are highly populated and of great economic and environmental importance. For the mean of accessibility of hinterland ports by large cargo ships, men influence estuaries on large scale (e.g. dredging), with that altering the behaviour of an estuary, e.g. the Western Scheldt (Swinkels et al., 2009; Bolle et al., 2010; Jeuken and Wang, 2010). Unfortunately, little is known about natural behaviour of the main shipping obstacles, namely shoals.

This research studied the development of an initial straight channel to an alternating bar-channel estuary system. The analysis of this research was conducted on the data produced from a tilting flume experiment, which contained two open boundaries for the production of a symmetrical tide. To investigate the development of the alternating bar-channel system, the first 2000 cycles of the experiment were analysed. Special attention was given to the dimensions of the bar-channel wave and the dynamics of the estuary bends.

The results presented in this study point to the existence of three consecutive periods, namely: the periods of chaos, growth and stabilization. During the short period of chaos, patterns were developed from the chaotic initial state, taking roughly 400 cycles. The following 800 cycles were characterised by the largest dynamics of the estuary bends, growth of the bar-channel wave dimensions and estuary width, called the period of growth. During the last 800 cycles, these dynamics and growths stabilize, except for the decreased growth of the estuary width. Moreover, a positive linear relation was found between the bar-channel wave amplitude and the width-depth ratio of the estuary. Furthermore, the outer bends were not influenced by the inner bends rejecting bar push theory for this experiment.

1. Introduction

1.1 Relevance

Coastal areas are among the most densely populated areas. With a rapidly growing population, especially in developing countries, the pressure on the natural systems is exceeding the environmental capacities. Particularly delta environments are susceptible to these developments.

As part of a delta systems, estuaries are of great economic importance due their connection between the sea and the hinterland ports (Hibma et al., 2004). But these systems are also showing a large biodiversity and are home to a dense human population. In order to sustain and supply the needs of all the "users", it is of great importance to know the natural behaviour. Although the morphological features are well known and the hydrodynamics of these systems is partly understood, the complex and critical interplay between these two is only poorly reported in literature. This and the large variety in time and space scales of these systems form large engineering challenges (Himba et al., 2004), especially with the ongoing climate change bringing human induced increase in rising sea levels (Barbier et al., 2011). The understanding of estuarine morphology could help to manage these environments more carefully and economically. If it is known how these systems behave naturally, this knowledge can be used to let the system itself "work" for these developments, for example in projects like building with nature.

In this research an experiment conducted in the metronome facility of the Utrecht University was analysed. Unlike estuaries in nature, the conducted experiment had two open boundaries at both sides of the channel to establish a symmetrical tide.

1.2 Thesis outline

The following paragraphs give a quick overview about what is already known about estuaries, followed by a conclusion pointing out which knowledge is still missing. Based on this knowledge the relevance of this study is emphasized and the hypothesizes are formulated. Chapter 2 gives an outline of the metronome, the conducted experiment, the data collection and the data processing. In chapter 3 the results are emphasized during three periods: chaos, growth and stabilization. These results are discussed and concluded in the chapters 4 and 5, respectively.

1.3 Research questions

The main research question to be answered by this research is: how do channels and banks evolve during the first 2000 cycles of the conducted experiment? This main research question is subdivided in the following sub questions:

- How does the wave length and amplitude of the longitudinal channel-bar waves develop during the first 2000 cycles?
- How does the estuary channel width develop during the first 2000 cycles?
- And how do the channel bends develop during the first 2000 cycles?

1.4 Literature review

1.4.1 Definitions

One of the most used definitions of estuary is given by Pritchard (1967). He defined an estuary as where seawater is measurably diluted by fresh water coming from the land. However, for morphological research the definition of Dalrymple et al. (1992) could better be used. They state the following: "we will define an estuary as the seaward portion of a drowned valley system which receives sediment from both fluvial and marine sources and which contains facies influenced by tide, wave and fluvial processes (Figure 1)". This definition is better for morphological research since it considers the morphological features to define the boundaries of the estuary, instead of the chemical composition of the water, which also changes on different timescales due to, for instance, the river discharge and tidal components. However, the conducted experiment of this research did not contain any river input. In order to overcome this definition problem, the following simplified definitions is used on the basis of Dalrymple et al. (1992): an estuary is the seaward portion of a

drowned valley system that receives and transports the same magnitude of sediments from both directions and is influenced by tidal hydrodynamics.

In order for a river to drown, the relative sea-level rise should be large enough to overcome the sediment delivery by the river and thus should be a transgressive system. However, the pace of drowning should be low enough in order to develop sedimentary features that are also influenced by river hydrodynamics. The point from which the relative contribution of the river energy is decreasing is called the apex and stated as the landward side of the estuary.

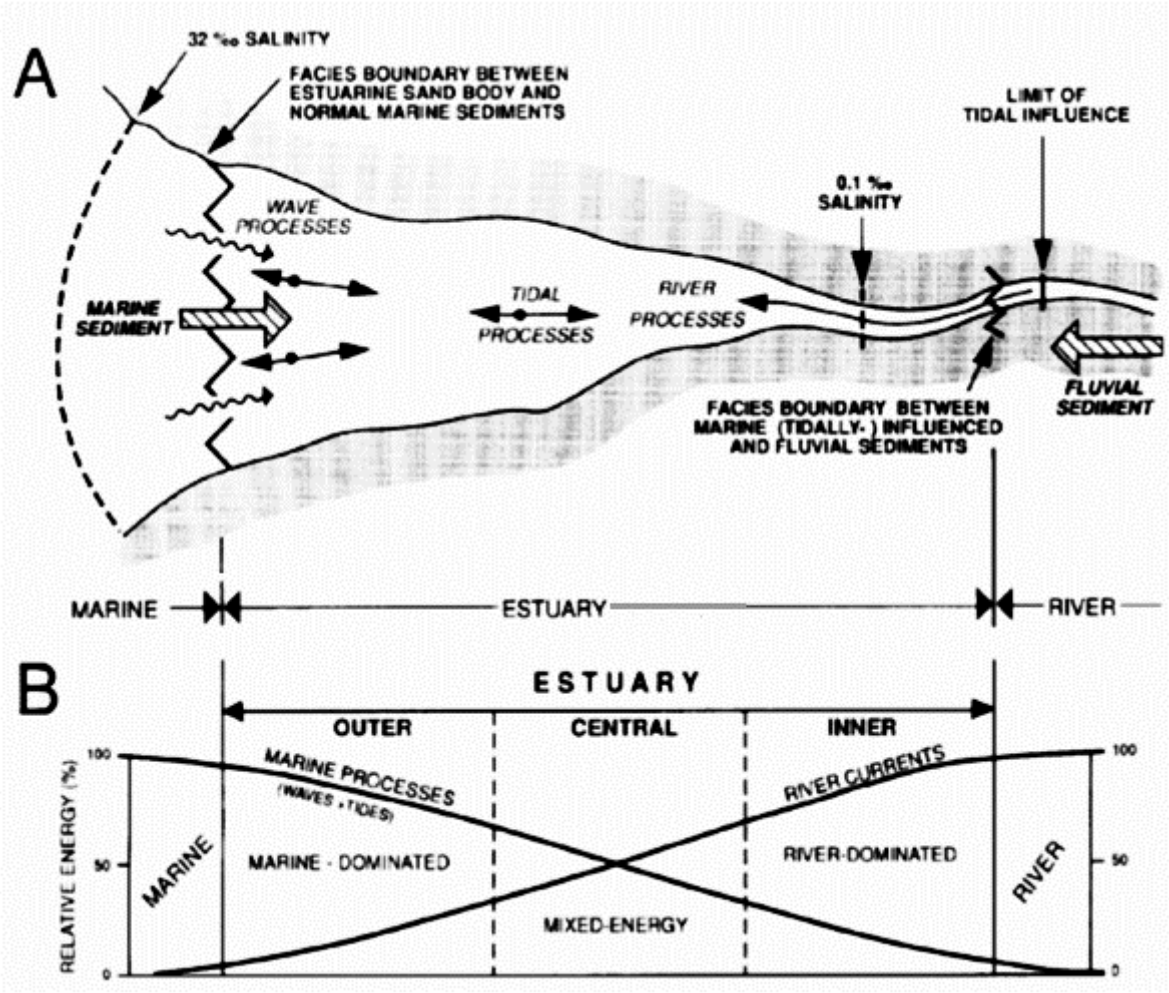

Figure 1 a schematic overview of an estuary and interplaying processes (A) and the relative importance of the processes (B) (modified after Dalrymple et al., 1992).

1.4.2 Tidal channels

The first to recognize the existence of ebb- and flood-channel of an estuary was van Veen (1950) defining them as: “a tidal channel mainly open for ebb(flood) and ending with a sill”. A stunning feature of ebb- and flood-channels is their mutually evasive character (Figure 2). This can be explained by the fact that both channels are transporting sand in their main flow direction. As a consequence, when an ebb- and a flood-channel meet, sand is transported from both directions, named by van Veen (1950) as the battle of the deltas. This results in a surplus of sediment and the creation of sill at this point. Such a sill obstructs ebb to enter the flood-channel and vice versa.

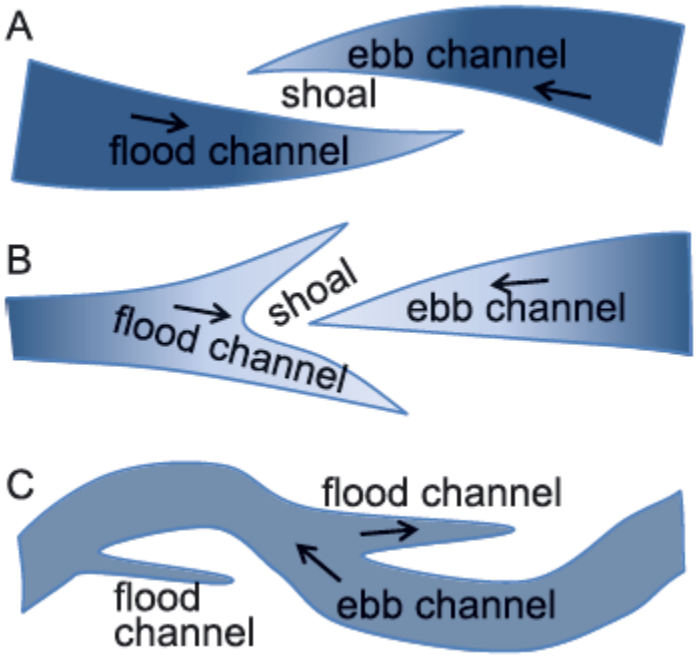

Figure 2 schematic representation of three mutually evasive ebb- and flood-channels (Kleinhans et al., 2015).

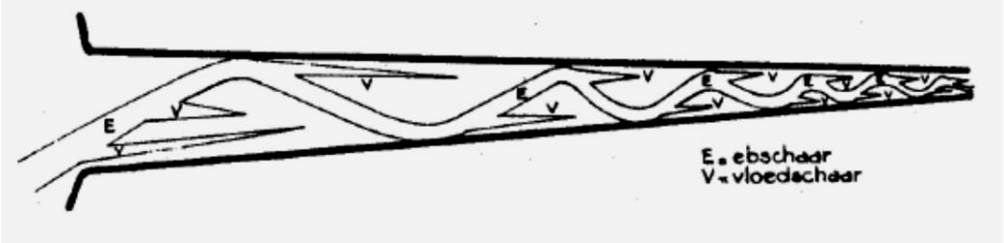

Figure 3 schematic representation of an estuary containing ebb- (ebschaar) and flood-channels (vloedschaar) (van Veen, 1950)

The schematic representation of the estuary the Scheldt (Figure 3), van Veen (1950) compared to a popular tree. In this case, the main stem was used as ebb-channel while side braches are flood-channels. But also Ahnert (1960) found a similar pattern around the Chesapeake Bay. He found that this pattern was best developed in the stretch of the estuary where the flow velocities were shifted in such a way that maximum ebb and flood are both at the same water level.

1.4.3 Tidal bars

Estuary bars are classified as simple unit bars and compound bars (Leuven et al., 2016). Unit bars are generally elongated, with a length between 100 and 300 meters. Their highest point is in the direction of the main flow (Leuven et al., 2016), resembling the river bar topography. Compound bars occur in a wide variety of shapes and sizes (Figure 4). These bars form due to different sedimentation and erosion processes, merging bars (Leuven et al., 2016). Erosion processes lead to the formation of barb channels (Figure 4h) on the compound bars. These barb channels are the estuary counterparts of chute cut-off channels. However, barb channels are usually less successful in crosscutting a bar. The reversal of the flow causes the “battle” of the deltas creating a sill at the end of the channel (van Veen, 1950).

Schramkowski et al. (2002) found that the combining effects of bottom friction and advective processes leads to the sedimentation (erosion) in the shallower (deeper) parts of the estuary. This positive feedback leads to the formation of estuary bars. They also found, with their analytical model, that the bar length increases with flow velocity and tidal excursion length. This is not confirmed by another analytical model by Seminara and Tubino (2001) or the numerical model of Hibma et al. (2003). Seminara and Tubino (2001) found the length of the bar to increase with

estuary width, while Hibma et al. (2003) found it to scale with the estuary width-depth ratio. These relations are also found in empirical research, the first for estuary bars (Leuven et al., 2016) and the latter for river bars (Kleinhans and van den Berg, 2011). Leuven et al., (2016) found this relation between bar length and estuary width on the basis of estuary satellite images. In order to do so, they broke down compound bars to their unit bar sizes. This resulted in the general founding that the estuary unit bar length is roughly equal to the estuary width and 7 times the bar width.

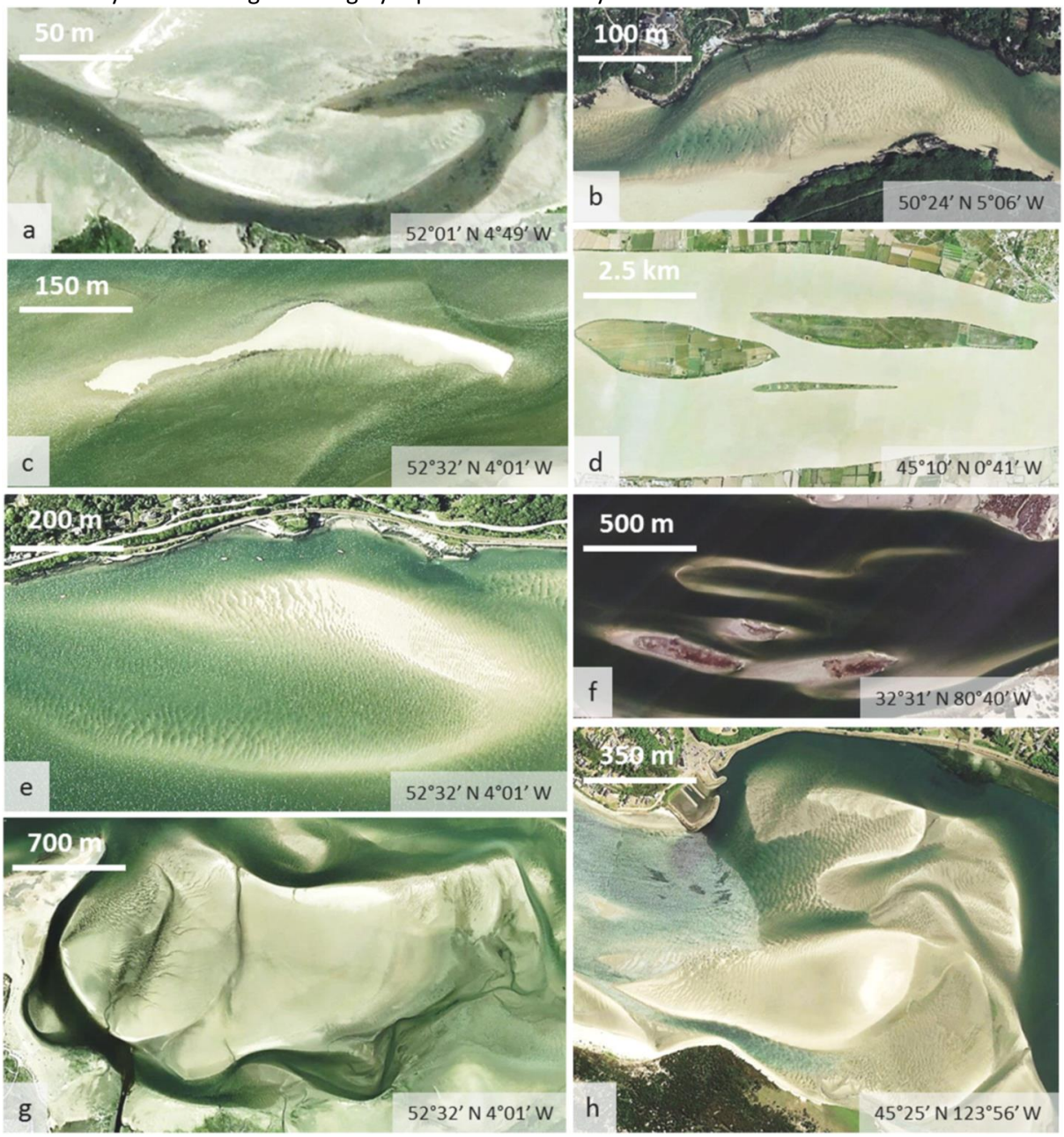

Figure 4 aerial photographs of different estuary bars (Leuven et al., 2016).

1.4.4 Estuary meanders

When an estuary is wide enough, roughly 3 to 5 times the main channel width, this channel begins to meander. These meanders will increase in size until a boundary is reached that decreases the erosion at the outer side of the meander (van Veen, 1950). The reversal of the flow causes the geometry of these meanders to be slightly different compared to their river counterparts. As can be seen in Figure 5, the reversal of the flow causes a sharp inner bend and a sand bar in the centre of the channel. Another difference between river and estuary meanders is the lower migration rate.

Due to the reversal of the flow, bar push effect is decreased, which is held responsible for river meander migration (Hoitink et al, 2017). Also the more cohesive sediments available in an estuary cause the low migration rates of estuary meanders (Kleinhans et al., 2009).

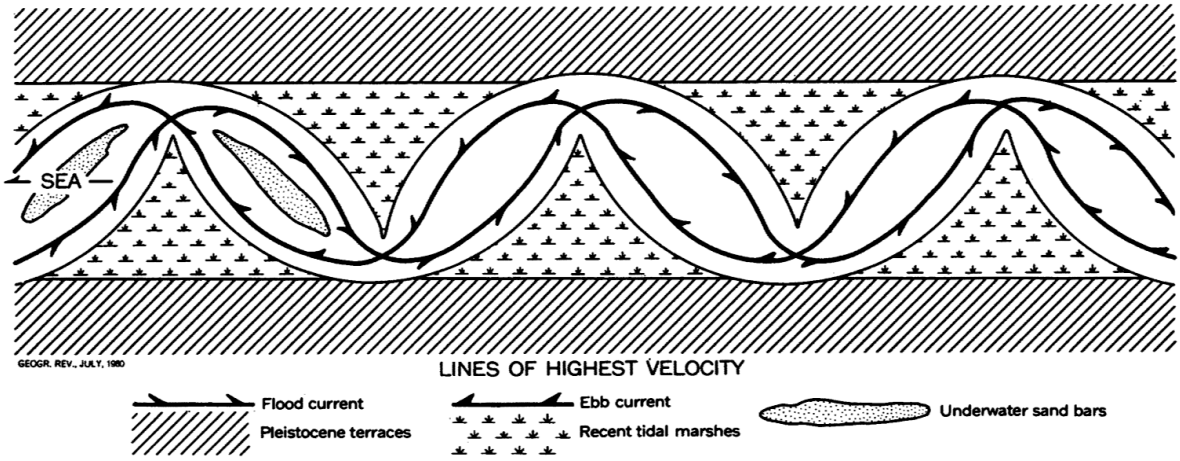

Figure 5 schematic diagram of estuarine meanders and flows (Ahnert, 1960).

1.4.5 River bars

In contrast to estuary bars, there is known a lot about river bars. In meandering rivers, the distinction is made between three types of bars: chute, scroll and tail bars (Figure 6). A chute bar is the result of an incomplete or failed chute cut-off. Due to the convergence of the flow at the end of the chute channel, flow velocities will drop, resulting in a deposition of the sediment and with that the creation of the chute bar. Tail bars are the result of debris stuck on the riverbed. This debris will block the flow, which results in a decrease in flow velocities behind it, causing deposition and growth of the bar.

Scroll bars are hypothesized to be the result of decreased flow velocities in the inner bend or bank pull theory. Both theories predict sedimentation of fine sediments just behind the apex of the inner bend, due to the decrease in flow velocities. The difference however is the cause of the decrease in flow velocity. Due to the inertia of the water, the thalweg of the river flow is deflected to the outer bend. This results in a decrease of flow velocities in the inner bend. However, according to bank pull theory, this is not enough for the creation of a scroll bar. Bank pull theory suggests that the deflected thalweg and the following erosion of the outer bend results in a widening of the channel. This widening of the channel decreases the flow velocity of the inner bend enough for sedimentation and the creation of a scroll bar (e.g. Eke et al., 2014; van de Lageweg et al., 2014). The counterpart of bank pull is bar push theory. Bar push theory explains the erosion of the outer bend with the growth of the scroll bars due to the deflection of the thalweg. The growth of the scroll bar narrows the channel, which results in an increase of flow velocities, mainly in the outer bend, and by that increasing the erosional capability at the outer bend.

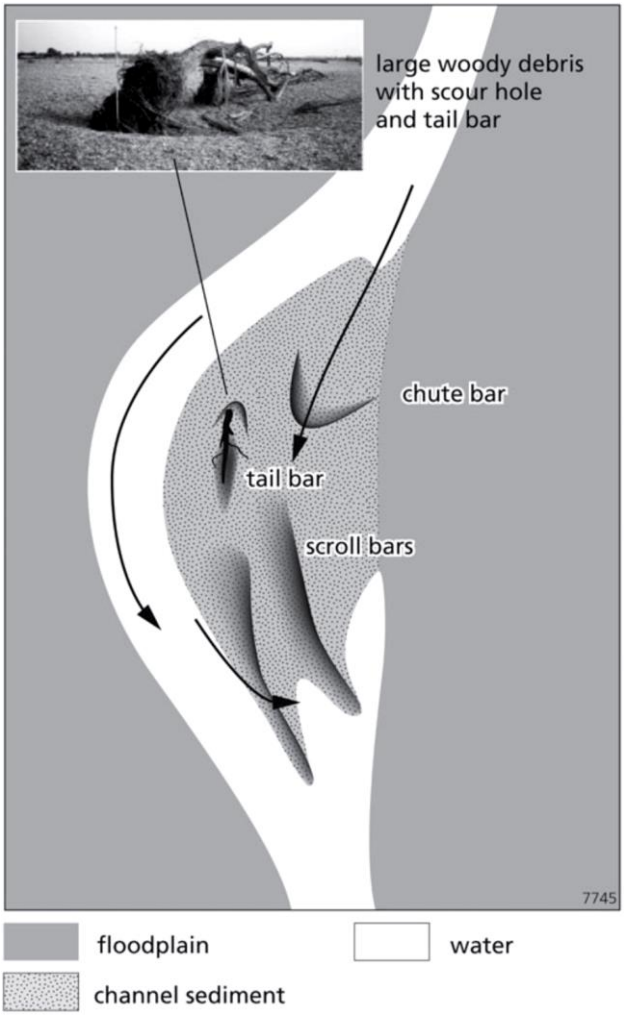

Figure 6 schematic figure of different types of river bars (Kleinhans and van den Berg, 2011)

1.4.6 Tidal flow

There are different drivers of water flow in an estuary. The water cycle of the landward directed current at the water surface and the seaward directed water at the bottom is called: the estuarine circulation. Jay and Musiak (1994) fount, based on their 2D model, that tidal straining is the main driving process behind the estuarine circulation. This tidal straining causes induced stratification during the ebb phase of the tidal cycle. Since the less dense, fresher river water flows on top of the denser, saltier sea water in the same direction, the vertical eddy diffusivity caused by turbulence to decrease. During the flood phase this is reversed, which leads to a reduction of the stratification (Simpson et., 2005). Due to the decrease in stratification, the velocity profile tends to be logarithmic during the flood phase. However, the increase in velocity with height during the ebb phase is more linear (see Figure 7). This causes the flow in the lower water column to be landward directed and the upper water column flow to be seaward averaged over a tidal cycle.

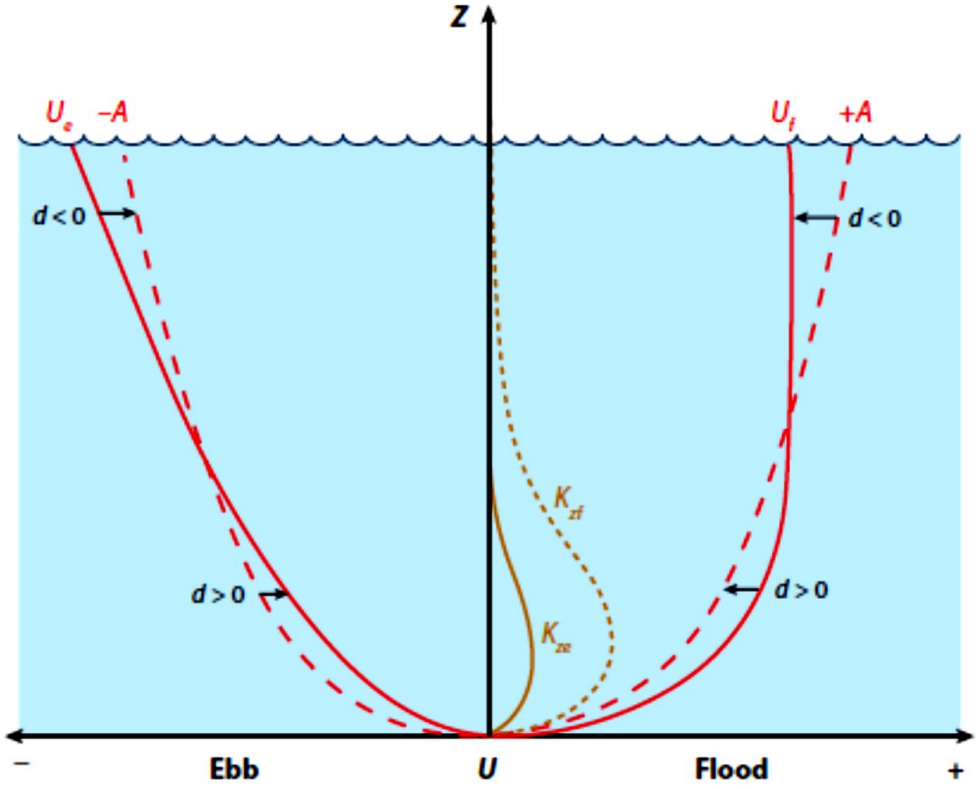

Figure 7 schematic representation of tidal straining of a single constituent. Lines indicated with A are the velocity profiles of perfect reversing single harmonic. U_e and U_f are respectively the ebb and flood velocity profile. K_{ze} and K_{zf} are the vertical eddy diffusivity caused by turbulence for ebb and flood. Indicated with d is the difference between A and U of which the sum is 0. (MacCready & Geyer, 2010)

Density currents driven by salinity gradients do also contribute to the flow in an estuary. Due to the lower density of the water at the landward side of the estuary, the water levels have to be higher in order to come to, approximately, the same total pressure as the seaward side. This causes a higher bottom pressure at the seaward side and a higher top pressure at the landward side (see Figure 8). The pressure difference in the water column results in a landward directed flow at the bottom, called the exchange flow (Geyer and MacCready, 2004) and a seaward directed flow at the top. By increasing these both flows, the velocity gradient will increase, and with that the internal shear stress (van Rijn, 1990). This tends to increase the mixing, decreasing the stratification and with that, decreasing the exchange flow.

When flow and water level are closely in phase, also stokes drift can transport water. This is caused by the fact that during high water, a larger water column is moved in landward direction than in seaward direction during low water. On the premises that both the ebb and flood velocities are approximately equal, this will cause landward directed flow (see Figure 9) that needs to be compensated by a return flow (Stokes, 1847).

In estuaries with distinct ebb and flood channels, tidal pumping can be an important contributor to tidal flow (Nguyen, 2008). Due to the ebb and flood channels, landward and seaward flows have less interaction, like pipes pumping the water in a circuit, thus resulting in a lower amount of mixing (Fischer et al., 1979).

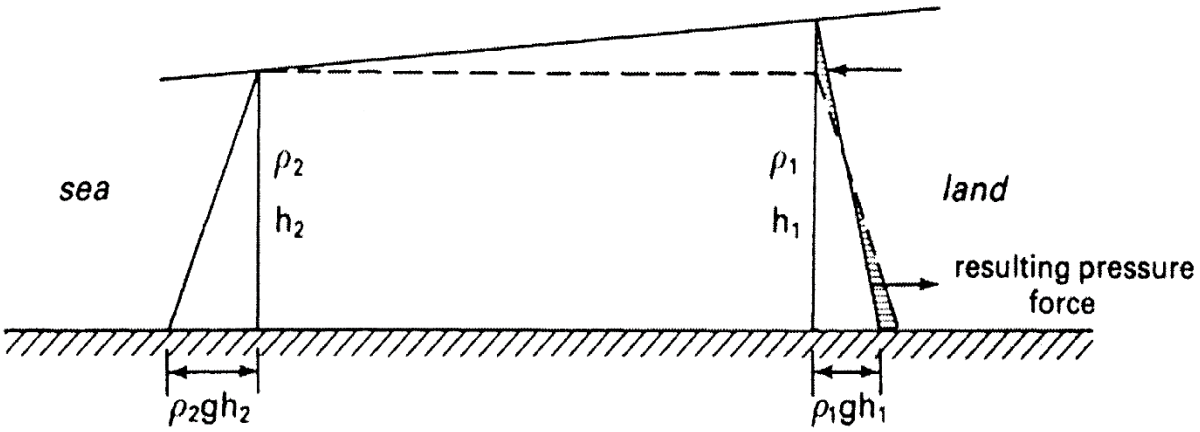

Figure 8 schematic representation of the fluid pressure in an estuary (after van Rijn 1990).

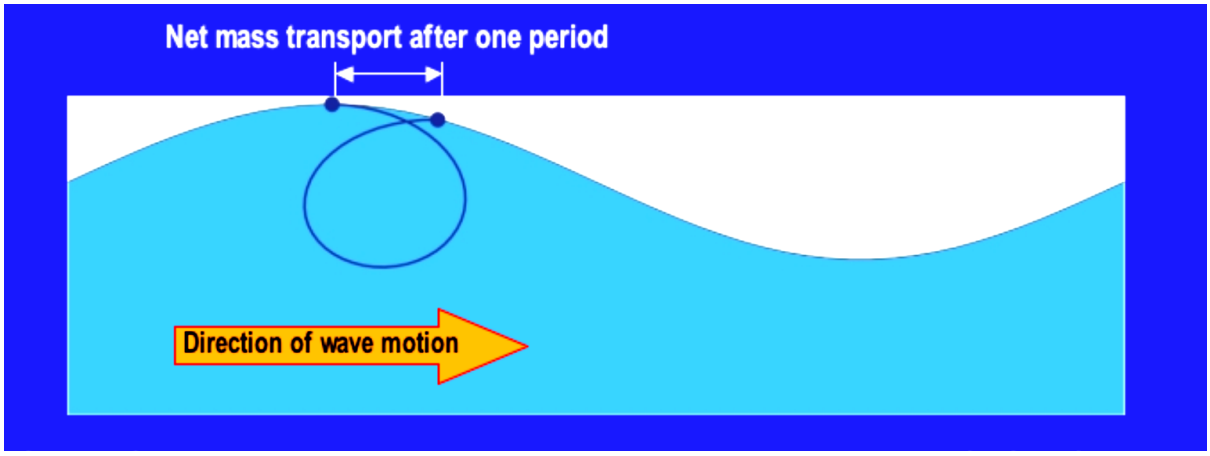

Figure 9 schematic representation of Stokes drift (after blogs.denison.edu).

1.4.7 Estuary scale experiments

The first to set-up an estuary scale experiment was Reynolds (1889, 1890, 1891). In his experiment he fluctuated the sea level of the water and added minor river flow. One of his observation was that there are different patterns in the experiments with and without river flow simulation. Without river inflow the experiment reached a static state, which is in contrast with the experiment using river flow. This could probably be explained by the fact that the river flow was strong enough to transport sediments, however the sediments were not transported bidirectional. The lag of this bidirectional transportation of the sediment made this experiment differ from a natural estuary.

Besides these pioneer experiments of Reynolds, there are five other publications found in literature that experimented with a fluctuating sea-level (Tambroni et al., 2005; Garotta et al., 2008; Kleinhans et al., 2009; Stefanon et al., 2010; Vlaswinkel & Cantelli, 2011). Most of these experiments evolved to a static situation, while a real estuary should evolve to a dynamic equilibrium. The first cause of this problem is the sediment size used. The transport of the sediment requires a very small grain size, however large enough to be non-cohesive and thicker than the laminar layer to prevent hydraulic smooth conditions and subsequently unrealistic large scour holes and ripples (Kleinhans et al., 2012).

Secondly, the fluctuating sea level on the scales used in these experiments cannot result in enough bed shear stress to cause tidal transport through the entire flume. The reason for this is that a tidal wave in a small scale experiments decrease faster in along channel direction than in a normal estuary due to the smaller water depth (Figure 10). As a consequence, the tidal flow is only capable

of transporting sediments in the most seaward section of the experiment. In river scale experiments this is solved by tilting the flume. However, in a tidal experiment this means that the bed shear stress during the flood phase is upslope, making hardly any sediment transport possible. In the ebb direction, the flow is only capable of transporting sediments during the last phase, caused by the nearly horizontal water level and the larger sloping sediment bed, like the emptying of a bathtub (Kleinhans et al., 2012).

Since the fluctuating sea level method is not working, an alternative method was developed (Kleinhans et al., 2012). In this method the flume was periodically tilted in order to have sufficiently strong flow to move the sediment, since the flood shear stress is not up-slope and the bathtub effect is decreased (Figure 10). Although, the tidal water level behaviour is different in a tilting flume, these estuary scale experiments are successful (Kleinhans et al., 2017b). The most important effects in these scale experiment is the bidirectional sediment transport due to the reversal of the flow.

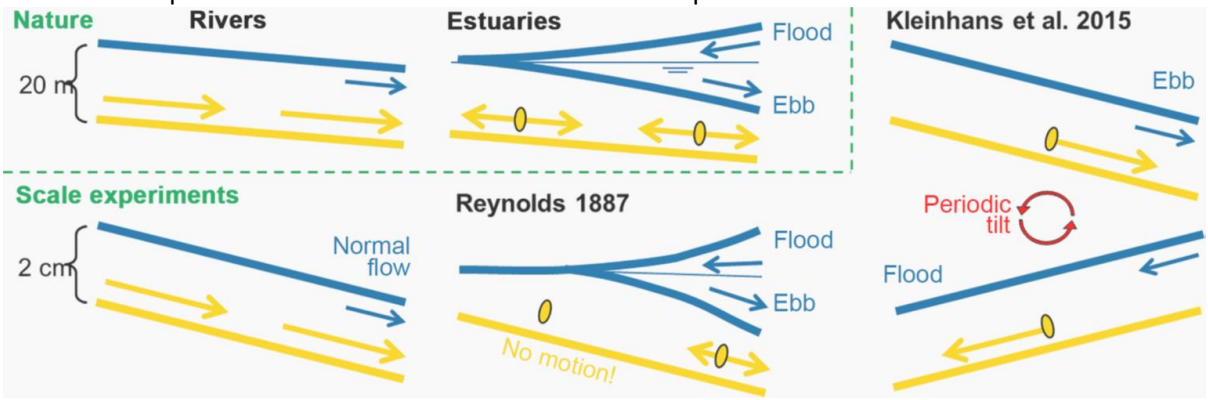

Figure 10 schematic representation of the behaviour of tide, tidal flow and bidirectional sediment behaviour in natural systems, Reynolds (1887) and Kleinhans et al. (2015) (Kleinhans et al., 2017b)

1.5 Gaps in knowledge

In morphological research there is a lot known about river and coastal systems. However, the knowledge where these two systems combine, an estuary, is lagging behind. Ahnert (1960) suggested that it is too fluviatile for marine experts and too marine for fluvial experts. It can also be attributed to the complexity of the system and the large range of scales, in time and space, that these systems evolve (Hibma et al., 2004). This is even further emphasised due to the fact that sediment modelling in 3D in reversing flow is not yet entirely understood and field observation spanning the entire systems time scales are not available (Kleinhans et al., 2017b), which is particular problematic for the larger time scales involved. This could be solved on the basis laboratory experiments. However, also this data is scarce (Kleinhans et al., 2017b).

As emphasized in section (section 1.4.6) there is some understanding of the hydrodynamics in estuary systems. This can be attributed to the fact, that this can be measured reasonably well, since the major changes in estuary hydrodynamics are on time scales up to a month. Also physics based modelling of hydrodynamics is well understood. Besides this, morphodynamic features are well documented. However, the link between the morphodynamics and hydrodynamics is only weakly known. This link is the major driver of the development and the adaption to changes of estuary systems. As a consequence, there is a lack of knowledge about the development of tidal channels, bars and bends.

1.6 Hypothesis of research questions

It is hypothesized that during the first couple of cycles, order in the systems cannot be seen, but will grow from an initial stage of chaos. From this point, estuary width will increase and with that the tidal discharge and flow velocities will increase due to the increase in tidal prism (Escoffier, 1977). Due to the increase in flow velocities the tidal excursion length will also increase. Based on literature the increase in flow velocity and tidal excursion length (Schramkowski et al., 2002) or the increase in estuary width (Seminara and Tubino, 2001; Hibma et al., 2003; Leuven et al., 2016) could

all potentially lead to an increase in bar length and so in bar-channel wavelength. It is hypothesised here that the increase in bar-channel wavelength is not solely controlled by the flow dynamics or the estuary width, but a complex interplay between both. The increase in the bar-channel wavelength will probably also lead to an increase in bar-channel wave amplitude and with that, the location of the estuary meander bends. It can be expected that the initial growth of the estuary features is largest during the early stages of growth, from this point the growth will decrease or a dynamic equilibrium will develop (Defina, 2003).

2. Methods

2.1 The experimental facility, the Metronome

The metronome (Figure 11) is an experimental facility build between 2014 and 2015 at the Utrecht University. This experimental set-up is a 30 m long, 3 m wide and 0.4 m deep flume that is able to tilt periodically. The metronome tilts with a period of tens of seconds up to an amplitude of 1.15 degrees. A longer tilting period results in higher flow velocities. At both sides of the flume there are end tanks containing a weir, this controls the seaward water height (Kleinhans et al., 2017b).

In order to stop the experimental channels clinging to the sidewalls, a surface is needed to be applied with a larger roughness than the viscous sublayer thickness, but smaller than the smallest bedforms (Kleinhans et al., 2017a). This is done by applying artificial grass at the bottom and sidewalls of the flume.

Figure 11 the metronome during another experiment (Kleinhans et al., 2017b).

.

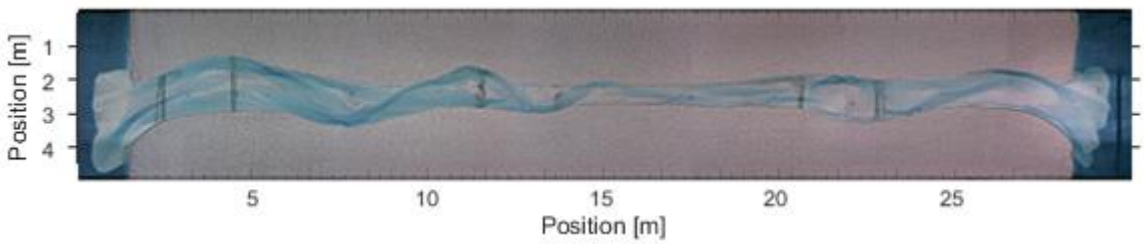

Figure 12 plan view image taken at cycle 900 during the experiment.

2.2 The experimental set-up

In this metronome experiment, two open boundaries are used (see Figure 12). This method is tested without sediments in the metronome by Kleinhans et al. (2017b). This resulted in in a nearly symmetrical reversing flow and thus a small scale estuary that is neither ebb nor flood dominant as can be seen in Figure 13. Flow velocities lag 2 to 3 seconds behind the tilting of the flume. It can also be seen that flow velocities are nearly equal for one phase through the entire flume. Also the water level is constant and static throughout the flume. The small water level fluctuations are causing only a minor overtides. The second overtide is only 2%, while the first overtide is even smaller (Kleinhans et al., 2017b). It can be expected that during the initial stages of this straight channel experiment the same tidal behaviour will occur.

In this experiment the amplitude of the tilting of the metronome was set on 75 mm with a period of 40 seconds. Sediment was characterised with typical value of 0.33 mm, 0.52 mm and 1.20 mm for the D_{10}, D_{50} and D_{90}, respectively and the water was dyed blue

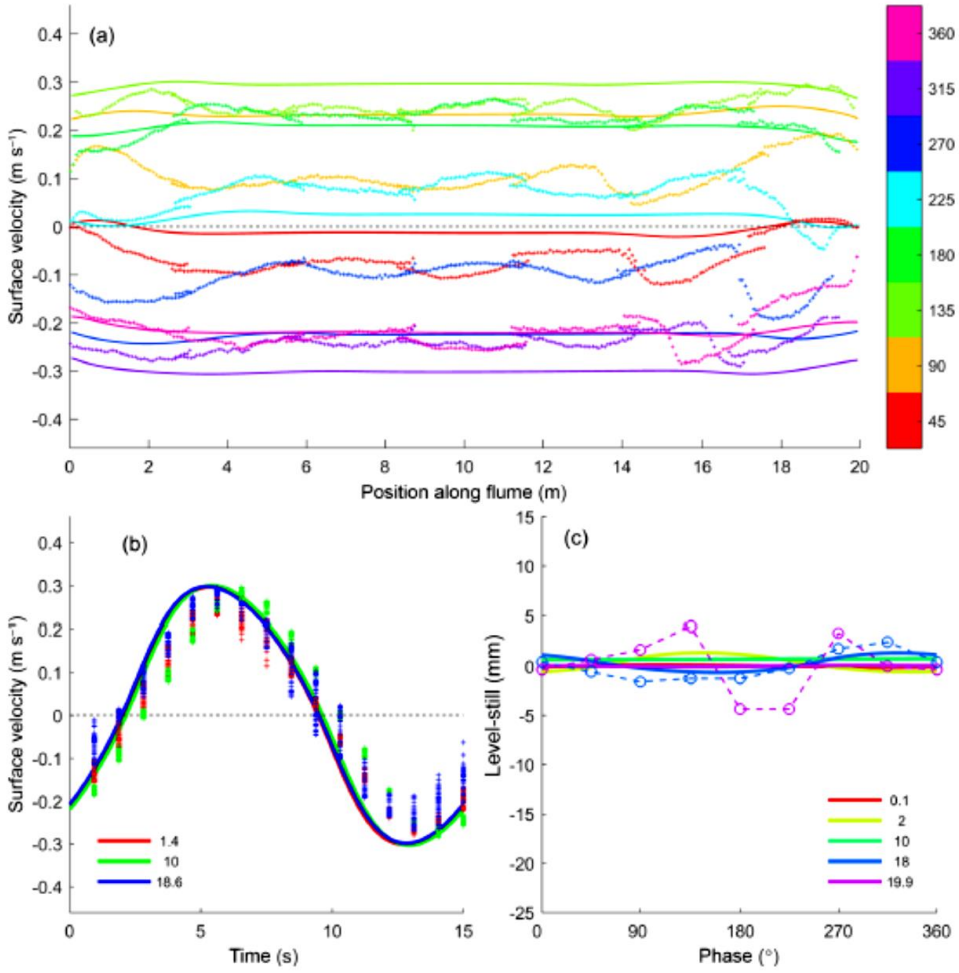

Figure 13 flow data of a two open boundaries experiment in the metronome, dots are used for measured data and solid lines for modelled data. (a) Surface flow velocities through the estuary per tidal phase. (b) Surface flow velocities for three selected locations through a tidal cycle (x = 0 at the start of the flume). (c) Water levels for five selected locations through a tidal cycle. (Kleinhans et al., 2017b)

2.3 Data collection and processing

During the first 900 cycles of the experiment the surface flow velocity was measured every 100 cycles using particle imaging velocimetry (PIV) using the same method as Blanckaert et al. (2012) and Marra et al. (2014). To obtain the PIV data, white plastic particles were spread over the water

surface by hand. These particles are captured with seven cameras, taking pictures at 25Hz, at the right moment in the cycle. For this experiment, PIV measurements were conducted for 16 different phases in the cycle. These cameras are mounted 3.7 m above the floor of the flume, spread with equal distance and have a 2048 by 2048 resolution. With a footprint of 3.15 m this results in roughly 1.5 mm/pixel. In order to calculate the flow velocities from the PIV measurements, the successive images were subtracted from each other. The difference between the successive images are the floating particles, from which the surface flow velocity can be calculated. Based on these images the bar-channel wavelength based on the river theory of Crosato and Mosselman (2009) could be calculated.

The same seven cameras also captured the flume every five cycles when it was horizontal. Due to the blue dyed water, these images could be used as a proxy of water depth. Firstly, the RGB values of the images were converted to LAB images (Figure 14). The B-band in these images indicates the yellowness/blueness of the taken images, higher values indicating yellow (colour of the sediments) and lower values indicating blue (colour of the dyed water) and thus lower values indicating deeper water.

The DEM measurements were taken every 100 cycles during the first 900 cycles. In order to do this, the flume was emptied and photographs were taken from a heighted frame in a horizontal angle. The location of the images in the flume was indicated with tags at the side of the flume every 2 m. These images were converted to DEM images with Structure From Motion. These DEM measurements were used to validate the qualitative depth measurements based on the LAB images.

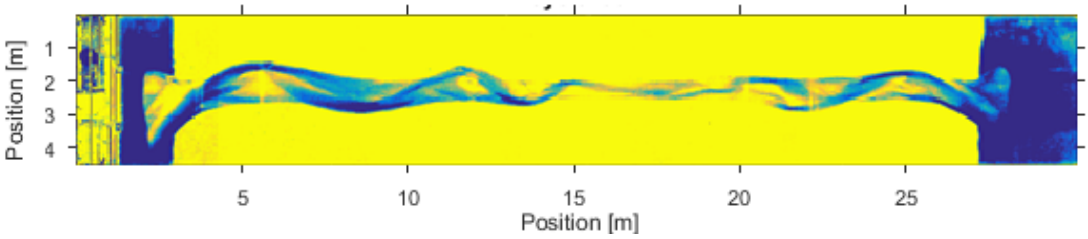

Figure 14 LAB images at the same cycle as Figure 12.

2.4 Experimental data analysis

During the analysis of the experiment, the experimental estuary was subdivided in two different segments, each containing an upper bank and channel, lower bank and channel and the middle channel, as can be seen in Figure 15. The segmentation was made since the left and the right part both behaved like an individual estuary, causing the development of the left part to be 200 cycles ahead of the right part. With the use of the segments, these two systems could be analysed individually. The location of the border was located on the part of the channel that only showed a minor grow in width and development of tidal bars and channels, marking the border of dominance between both open ends. The cross-sectional segmentation of the channel was subdivided with equal distances between both banks. The upper and lower bank were detected using the cross-sectional derivative of the blue value after smoothing the image (see Figure 16). As can be seen, the first pixels deviate from the bar. This is caused by the rolling mean to smoothen the border. Due to this deviation, these pixels are not used in the analysis. The smoothing of the borders was done in order to overcome unrealistic changes due to outlier LAB values. The first and last high absolute derivative indicated the upper and lower bank of the channel. The next border was placed on ¼ of the distance between the upper and lower bank, which is also used as the width of the channel. The borders were also used for the time space diagrams. For these figures, the 50 pixels around this border were averaged to fade measurement inaccuracies due to minor light changes.

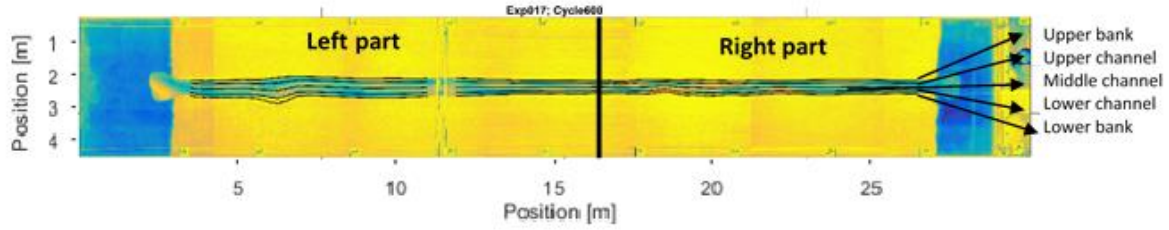

Figure 15 example of the segmentation during cycle 600 of the experiment.

Also the bar-channel wave length and amplitude were analysed. This was done for the upper and lower channel. Firstly, an along channel cross-section was detrended with a mean around 0 (see Figure 17). Secondly, for the bar-channel wavelength, it was detected if the first zero crossing was from positive to negative or vice versa. From that point the space difference between the next same type of zero crossing was measured. For the amplitude the peaks and crests were indicated, measured and subtracted to calculate the amplitude. It was chosen to analyse the bar-channel wave amplitude instead of bar height, since the bar-channel wave amplitude is not dependent on water level and this system is characterised by an alternating bar system revealing wave like patterns. Both the bar-channel wavelength and amplitude values were averaged over the entire channel, right and left part for one measured cycle.

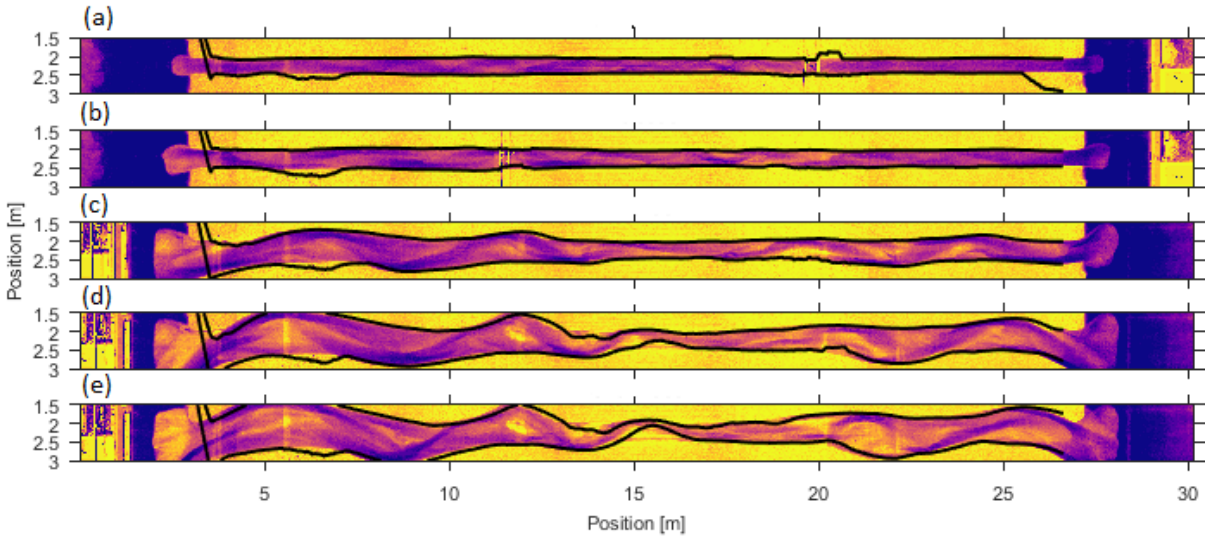

Figure 16 bank detection of the upper and lower bend for cycle 250 (a), 500 (b), 1000 (c), 1500 (d) and 2000 (e), the black lines indicate the upper and lower bank of the model results.

For the bend results, firstly the along channel bend locations were manually detected from the moment the bends could be clearly indicated by eye. Secondly, the cross-sections of these locations were made through time. In order to calculate the inner and outer bank migration at the bends a blue value was chosen visually such that both the inner and outer bank crossed. Lastly, the change in the position of crossing during 100 cycles was calculated. By using periods of 100 cycles the mean of the migration was identified, removing large jump sudden changes in the bank (e.g. slumps of the banks).

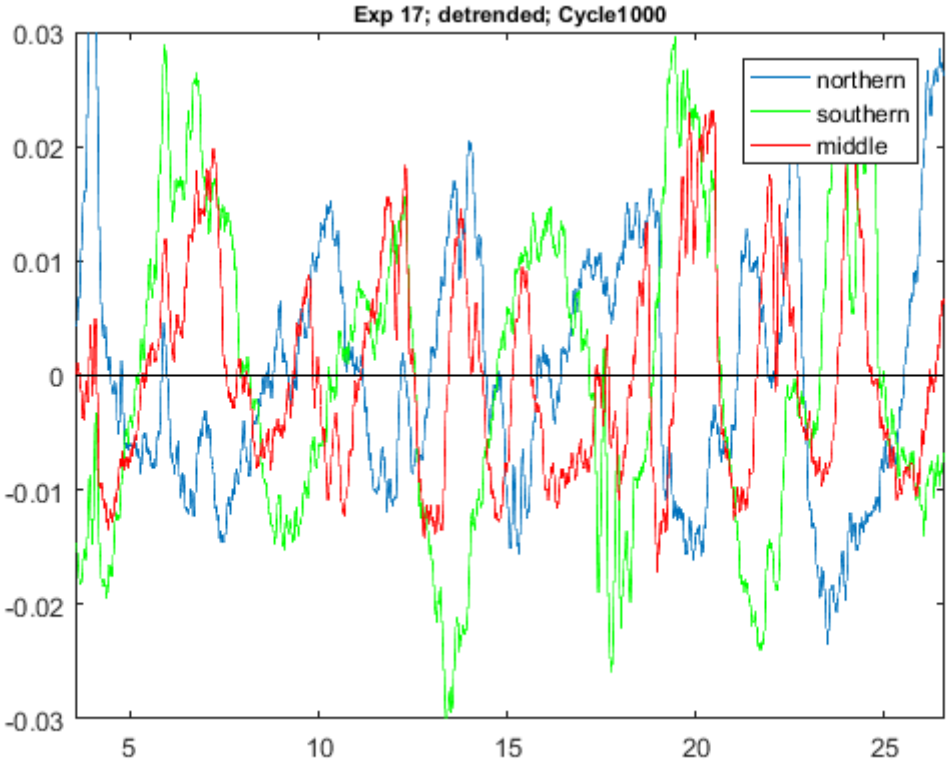

Figure 17 detrended bar-channel wave through the estuary during cycle 1000

3. Results

The conducted experiment and the results can be roughly subdivided into three different periods with small overlapping periods depending on the location in the channel. The first period is called the period of chaos and lasts until cycle 400, were it disappears in the middle of the channel. During this period, patterns are hard to observe or are slowly developing. The following period is called the period of growth. During this period the patterns and features developed during the period of chaos show the largest growth and dynamics and lasts until cycle 1200. The last period, thus lasting until cycle 2000, is called the period of stabilization. Some features show a small decrease in size at the beginning of this period, due to overshoot in the period of growth. The rest of this period is characterized long term averaged stable bar sizes, stagnant bends and a decreased growth of channel width.

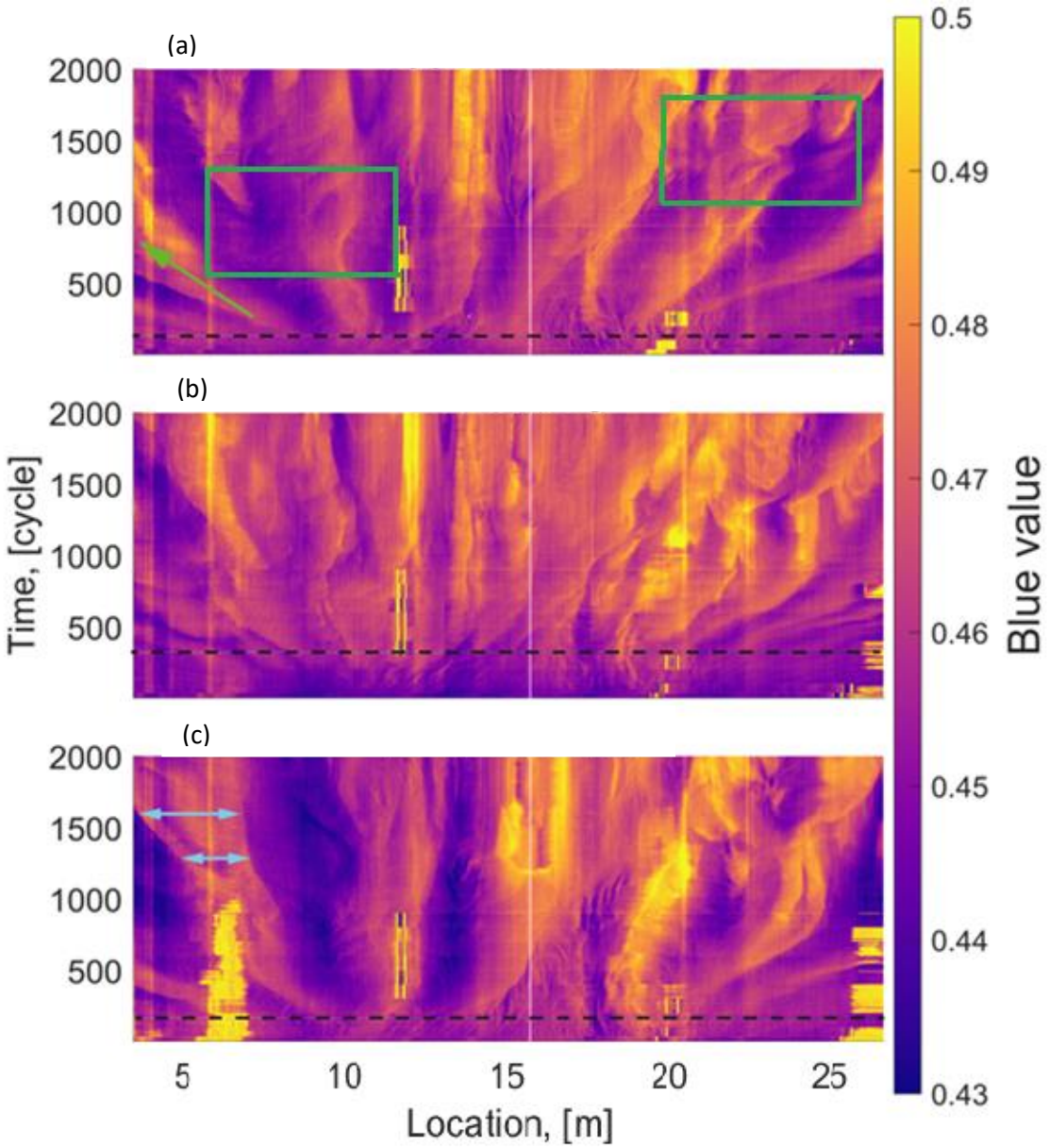

Figure 18 LAB value (quantitative indication of water depth) of the upper channel (a), mid estuary (b) and lower channel (c) for the first 2000 cycles, showing bar development, migration and erosion for the middle of the estuary, upper and lower channel (see Figure 15). Lower blue values indicating deeper water. Recognition of the first pattern Is indicated with the black dashed line. Bar development is indicated with the green boxes. Bar migration is indicated with the green arrow. Bar length growth is indicated with the blue arrows

3.1 Period of chaos

During the period of chaos there are no clear bars visible and bends in the initial straight channel are not yet developed. This can best be seen in Figure 18 were, until the end of this period, indicated by the black dotted line, there is no clear difference between high and low blue values but a blurred combination.

During this period, the bar-channel wavelength (divined as the distance between the top of two successive bars) and amplitude (divined as difference in bluevalue or height between the top of the bar and the longitudinal successive depth of the channel) are identified as can be seen in Figure 19 and Figure 20, respectively. This is in contrast with the observed blue values during this period in Figure 18, were this distinction between bars and channels cannot be seen. Both parameters show a small decrease in size during these first 200 cycles, indicating that the bar size with the highest growing rate is smaller than the average bar created by the chaos.

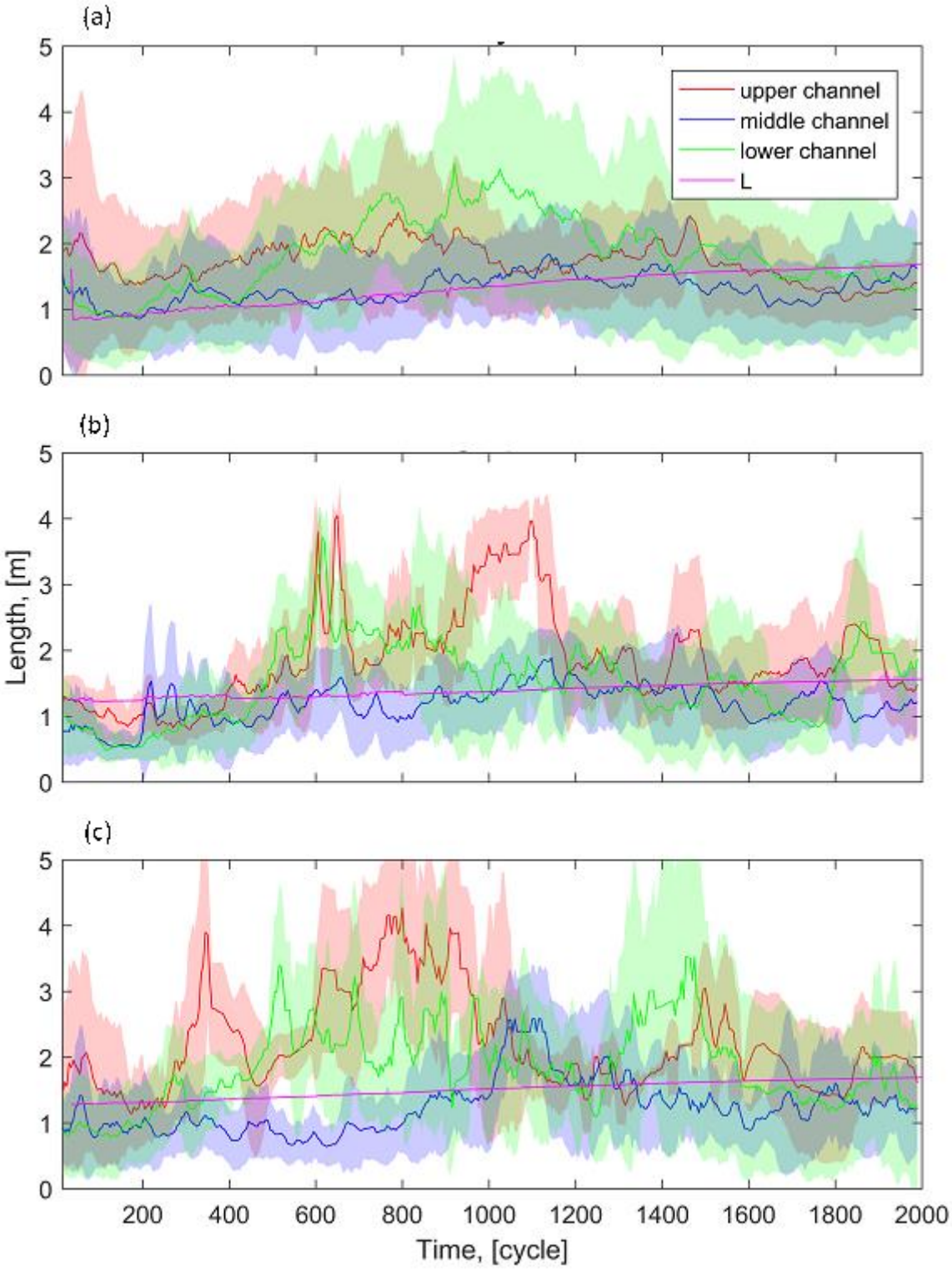

Figure 19 the along-channel mean of the wave length of the bed and associated standard deviation (shaded area) of the middle of the estuary, upper and lower channel through time of the entire system (a), right (b) and left part (c) (Figure 15). The purple (L) is the predicted wave length using the method of Leuven et al. (2016).

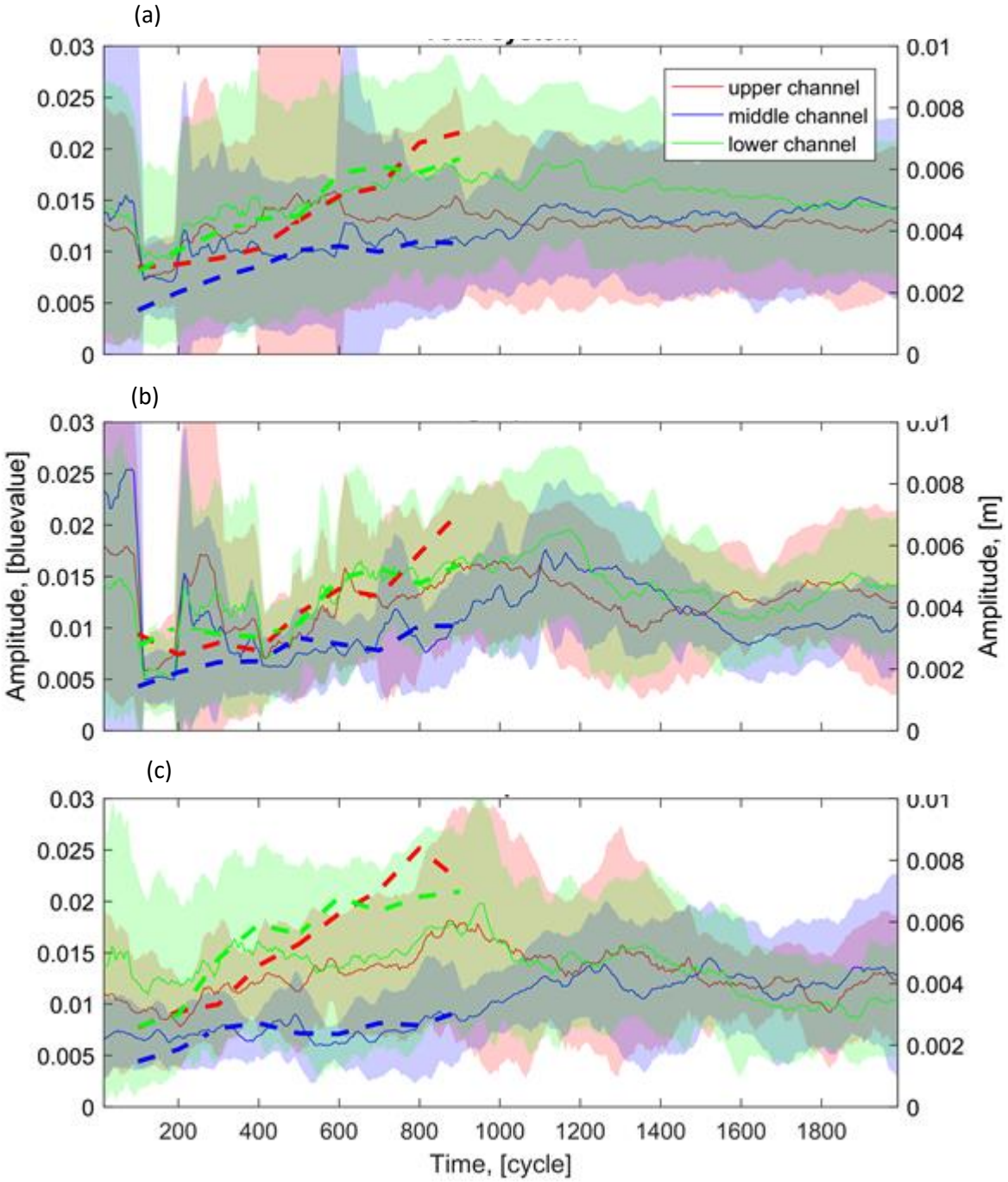

Figure 20 along channel mean wave amplitude of the bed and associated standard deviation (shaded area) of the middle of the estuary, upper and lower channel through time of the entire system (a), right (b) and left part(c) based on the blue value (thin, solid line, left y-axis) and DEM images (dashed line, right y-axis).

During the period of chaos, it can be expected that the standard deviation is highest and will show a decrease towards a more stable size. Although, not as clear as could be expected, this decrease in standard deviation can be seen in in Figure 19 and Figure 20 for the bar-channel wavelength and amplitude, respectively. This can however not be traced back in the bar-channel wavelength of the right upper channel, amplitude of left middle channel and the entire amplitude of the right part of the channel. The absence in this last one can be probably be attributed to an analysing error, since an unrealistic large jump is made in the amplitude and standard deviation.

The development of a bar-channel patter in the middle of the channel lags behind, roughly 150 cycles, the upper and lower channel. This can most clearly be seen in Figure 18 as is indicated by the black dotted line. This can be explained that the bars grow as side bars, as can be seen in Figure 21. In cycle 250, the bars do no reach or only just reach the middle of the estuary. However, during the following cycle the transverse growth caused the bars to cross the middle of the estuary in cycle 500. Since the existence of the bar is essential for the recognition of the bar-channel pattern, this causes recognition in a later stage in the middle of the estuary.

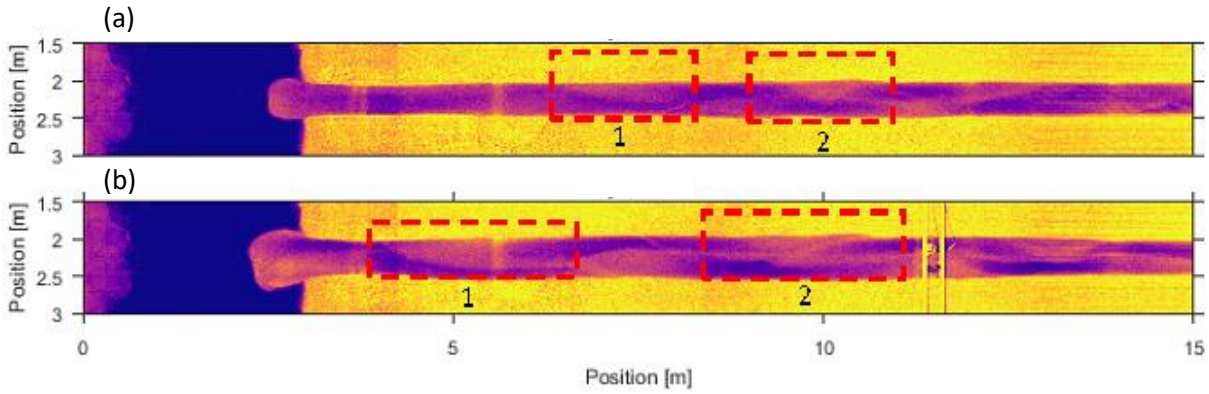

Figure 21 overhead image of cycle 250 (a) and 500 (b). Bar 1 and 2 are indicated during cycle 250 and 500 with the red dashed boxes

3.2 Period of growth

The period of growth is the most dynamic period analysed. In Figure 18 this can be seen by the large migration of the bars of which an example is indicated by the green arrow. Beside the migration, the dimensions of the bars and channel also increase. The increase in bar height is also indicated with the green arrow, showing an increase in blue value, indicating a decrease in the water depth and thus an increase in bar height. The increase in bar length can also be see in Figure 18 with the increase in width of the high blue value strokes. For an example, although not in this period, see the blue arrows.

During the first 1200 cycles, the increase in width of the estuary is largest (see Figure 22 (a)). Although a 100 cycle periodicity until cycle 1000, this can also be seen in the average gradient of the channel width over time during this period (see Figure 22 (b)). This periodicity can be attributed to the fact that the experimental set-up was emptied every 100 cycles until cycle 900 to conduct DEM measurements. This probably results in a small offset of the width in a short time, which comes in sight when calculating the width derivative. During this period the width difference between the left and right part also increases. The first difference is a step-like increase and decrease of the width of the left and right part, respectively. The rest of this period, the difference increased at a constant pace.

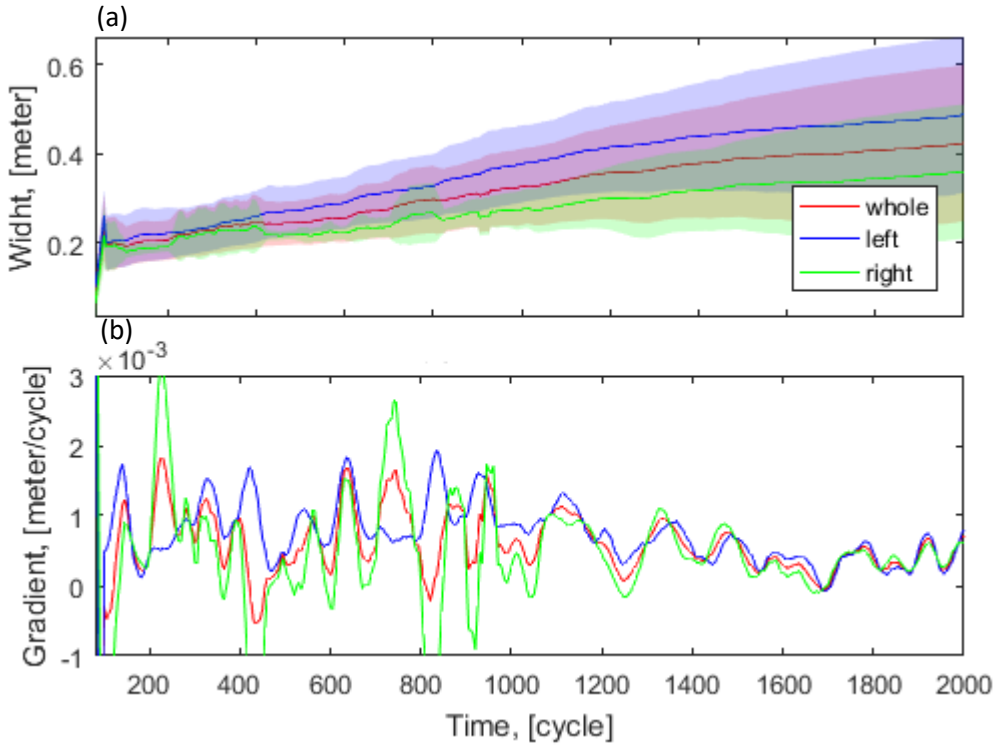

Figure 22 mean estuary width and associated standard deviation (shaded area) of the entire, left and right part of the estuary (a) and the change in mean estuary width over time of the entire, left and right part of the estuary (b).

Also the bar-channel wave length increases during the period of growth following the increase in estuary width (see Figure 19). Leuven et al. (2016) already found that the bar length in natural systems are expected to be equal to the width of the estuary. On the premises that the bar length is half the bar-channel wavelength, the width of the estuary is doubled to predict the bar-wave length with the method of Leuven et al. (2016) (purple line Figure 19). It can be seen that this gives an indication of the bar-channel wavelength. However, the method of Leuven et al. (2016) fails to predict the short term changes. Combined with the increase in bar-channel wavelength, also the amplitude increases, marking a general increase in bar dimension (see Figure 20).

During the period of growth, short term periods of large growth in the upper and lower channel of the bar-channel wavelength can be identified (see Figure 19). The beginning of these periods can be correlated with the migration of the bar out of the estuary (for example see dark green arrow in Figure 18). While the end of these periods can be correlated with the development of a new bar (for example see the green boxes in Figure 18). Due to the migration of a bar out of the estuary, the number of bar-channel waves will decrease, while the length of the estuary is equal. This results thus in an increase of the average bar-channel wavelength. However, this increase in bar-channel wavelength also creates more space for the development of a new bar between the existing bars. This increases the number of bar and thus decreasing the average bar-channel wavelength. These short-term changes cannot be traced back in the bar-channel wave amplitude, marking that these changes are not caused by an increase in bar dimension but rather by the developing of free space.

The migration of the channel bends also shows the largest dynamics until cycle 1200 (see Figure 23). This could be expected since the bends are located at the deep part of the bar-channel wave in the upper and lower channel. For the bar-channel wavelength to increase, the distance between the bends need to be increased and thus for a larger increase a higher migration is needed.

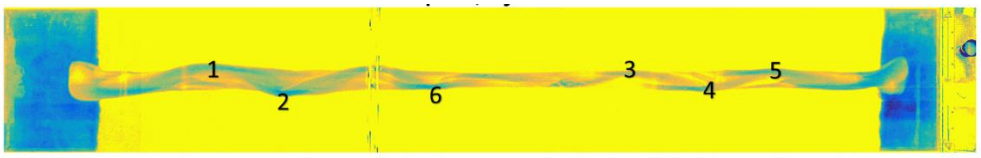

Figure 23 location and numbers of the bends tracked during the analyses of the experiment at cycle 900.

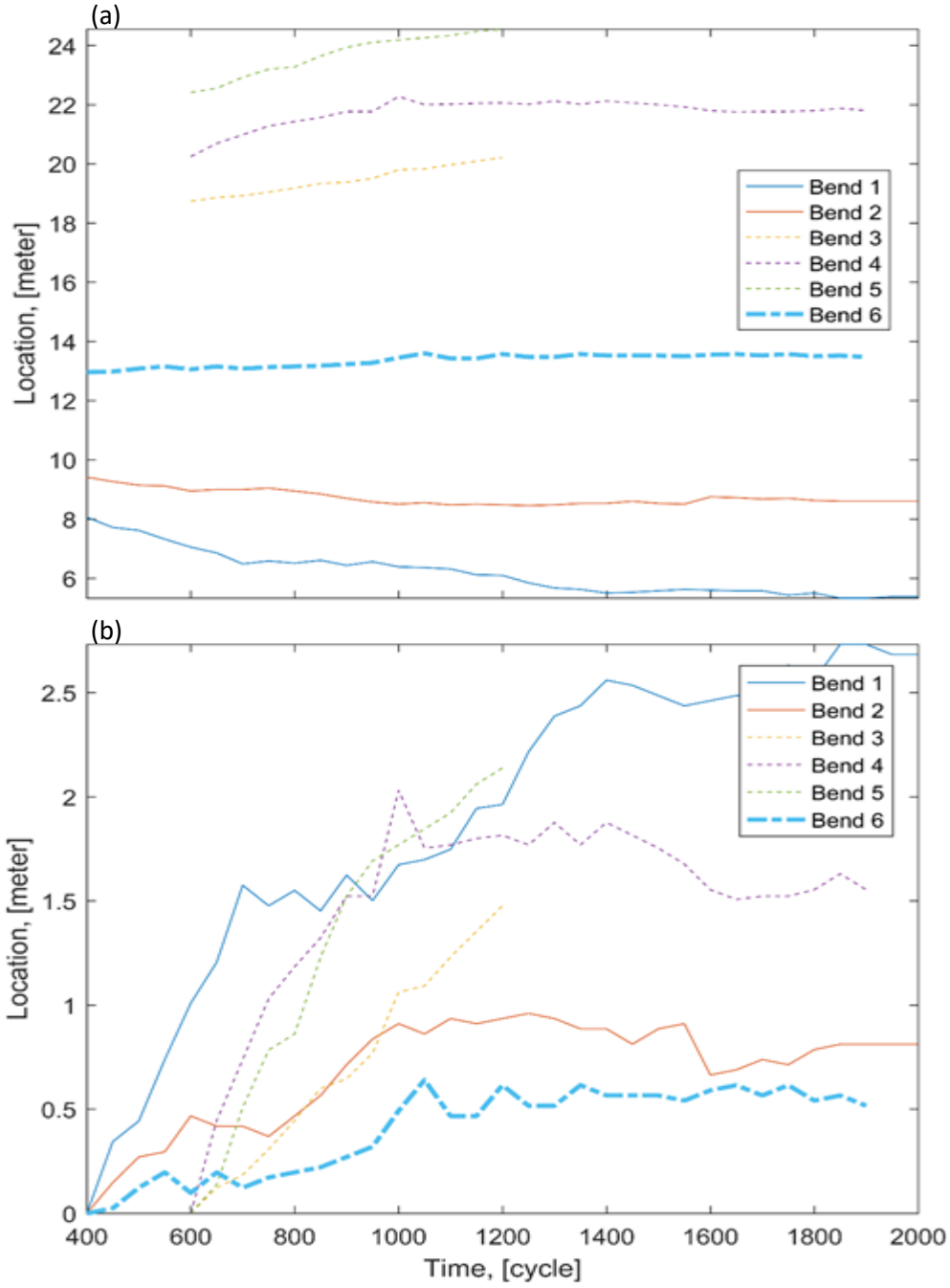

Figure 24 (a) position of the tracked bends over time. Colours are indicating bend number, solid lines are indicating bends in the left part of system, thin dotted lines the right part of the system and thick dotted line the middle of the system. (b) Relative bend position through time, location = 0 meter is the begin position from the start that the bends are tracked.

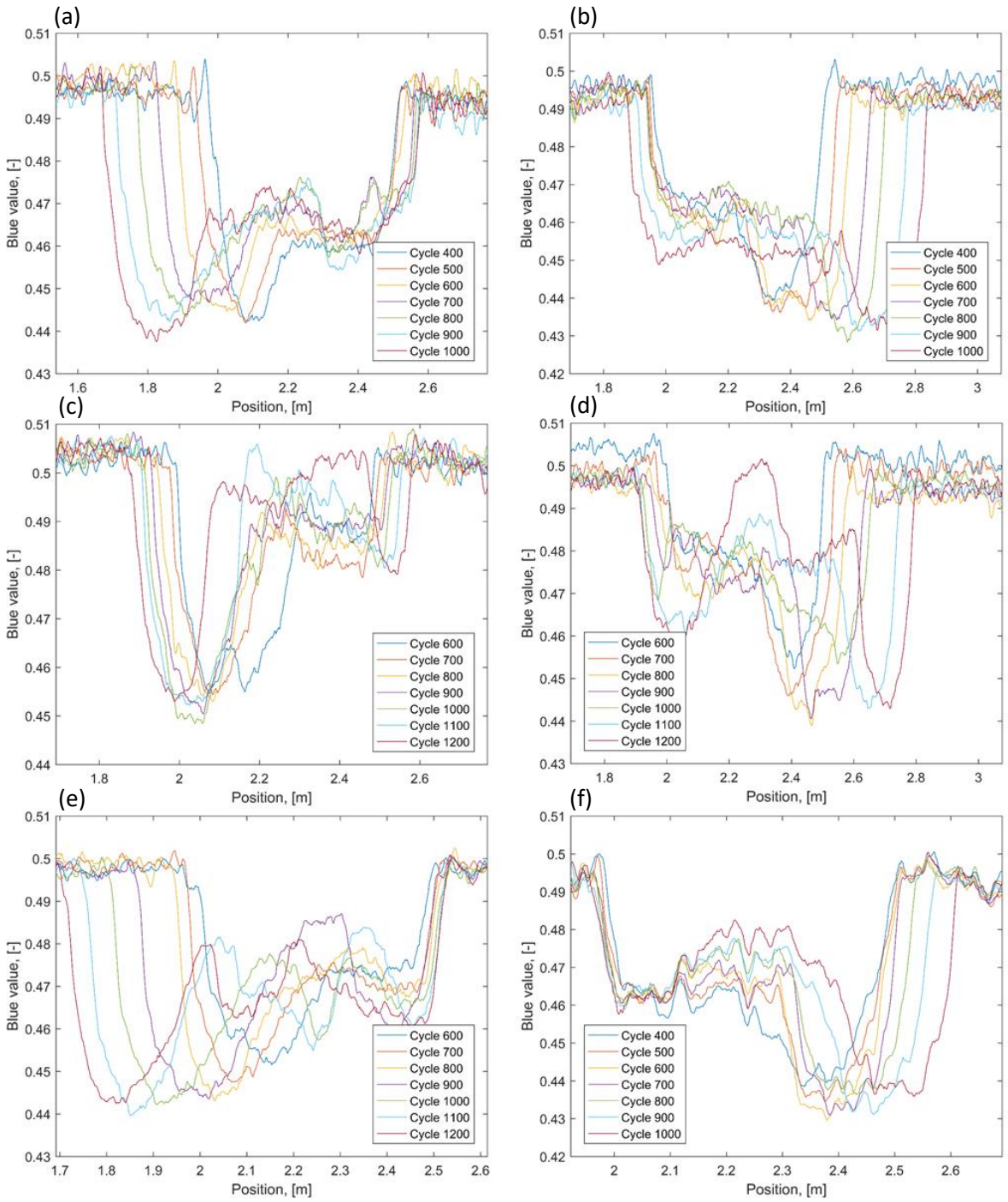

Figure 25 cross-sectional bed evolution of bend 1 (a), 2 (b), 3 (c), 4 (d), 5 (e) and 6 (f), colours are indicating the cycle.

The migration in the bends on the seaward side of the estuary are largest (see Figure 23 for the bend locations and Figure 24 for the migration). This can also be seen in the migration of the deeper parts of the channel in Figure 18. After an initial migration of bend 1 and 2 both bends show a small period without migration. This period lasts until the other bends in the same propagation speed class have reached the same migrated distance. In order to increase the bar-channel wavelength of the most middle wave, the subsequent bar-channel wave has to migrate slightly seaward. For this bar-channel wave to increase in length, the following bar-channel wave also has to migrate slightly combined with the slight migration needed for the middle bar-channel wave. This results in an increase of migration speed from the mid estuary bends to the seaward bends (see Figure 23).

During the period of growth, the transverse migration of the inner and outer bend differs in speed and constancy. From the transverse cross-sections of the estuaries at the bend locations it can be seen that the width of the estuary increases due to the faster migration of the outer bank compared to the inner bank (see Figure 25 and Figure 26). From Figure 26 it can also be seen that the outer bend displays a constant displacement through time, while the displacement of the inner channel can better be described as a step like migration. The constant change in outer bend position reveals that this is not influenced by the more chaotic change in location of the inner bend. If this was the case, the outer bend would show a similar step like location change, possibly with some delay. Since the outer bend is not influenced by the inner bend, it can be concluded that in this system bar push theory does not hold.

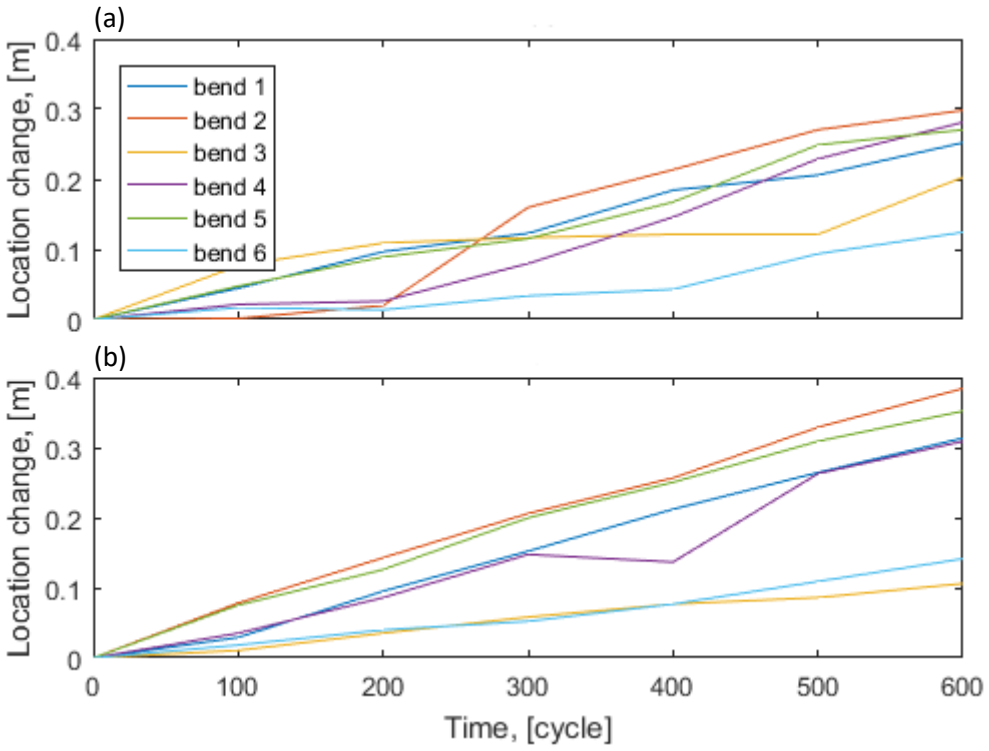

Figure 26 the cross-sectional displacement of the inner bend (a) and outer bend (b) through time as can be seen in Figure 25. Time = 0 and location = 0 is the first cycle and location of recognition of the bend.

3.3 Period of stabilization

The period with the lowest dynamics is called the period of stabilization. As can be seen in Figure 18 the migration of the bars (the yellow patches are more vertical), the change in water depth indicated by the blue values (the vertical patches show have a more even colour) and the growth of the bar length (the vertical patches are more constant in width) all decrease from roughly 1200 cycles onwards.

The only feature that shows an increase in change is the increase in the standard deviation of the width of the estuary (see Figure 22). Also the width keeps expanding during this period, however slower. The standard deviation of the width is a measure about the differences in width through the system. This difference in width through the channel can be explained by the decrease of the e-folding length scale and the increase of the quasi periodic widening and narrowing of the estuary described by Leuven et al. (2018). The increase in width of the left and right part of the system become more equal compared to the period of growth and thus shows a constant difference in width. This can also be seen in the gradient of the width through time, which is more equal compared to the previous period.

After the initial growth, it can be seen that the bar-channel wave length and amplitude both show a minor decrease, especially visible in the upper and lower channel, from which both become more stable (see Figure 19 and Figure 20). This is mostly visible in the separate analysis of the left and right part of the channel. When both parts are combined, this effect is blurred. This overshoot indicates an abrupt change in condition or the change from positive to a negative feedback of which an equilibrium is not yet found. After the overshoot of the bar-channel wave length and amplitude, both features do not show a long-term averaged growth. This indicates that the dimensions of the bar do not increase anymore.

3.4 General relations

By the comparison of the bar-channel amplitude based the bluevalue and the DEM measurements, it can be seen that the blue value is reliable proxy for the topography of the estuary channel (see Figure 20). This is of great importance since the resolution and frequency are higher and timespan longer for the bluevalue measurements. This improves the topography related visualization through time. Also, the DEM measurements require an emptied bed and are made manually. It can be expected that the emptying of the bed will influence the system, which is not desired.

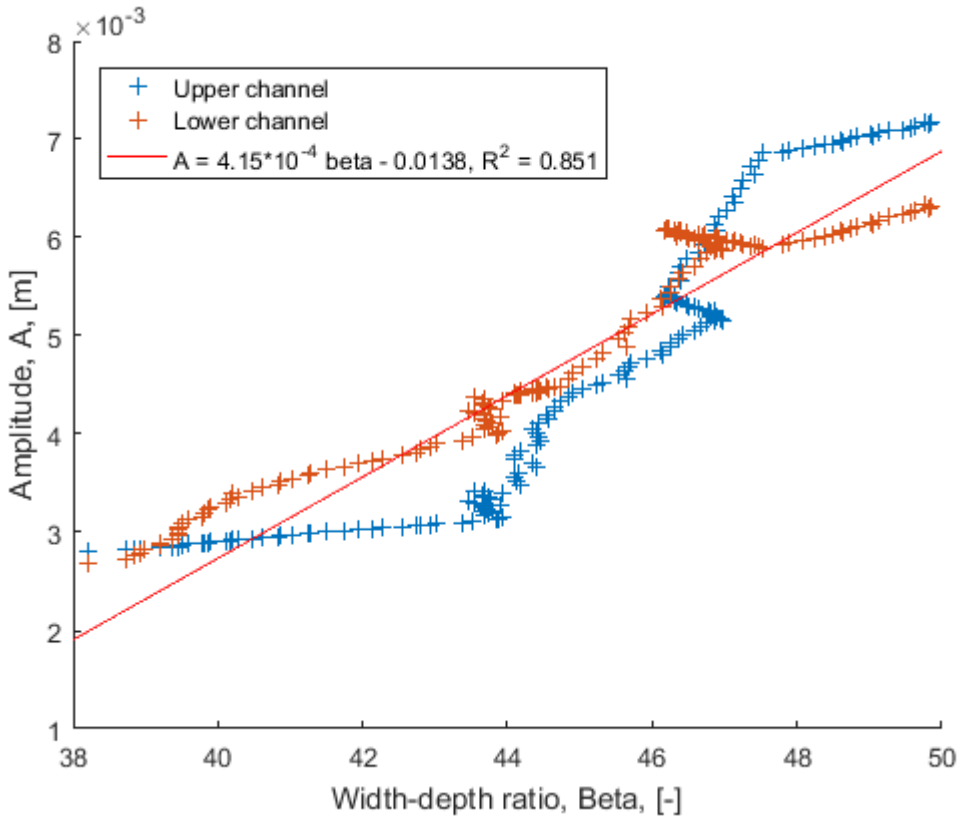

Figure 27 relation between the along channel mean bar-channel wave amplitude of the bed and the along channel mean width depth ratio for the upper and lower channel based on the DEM data, including regression line.

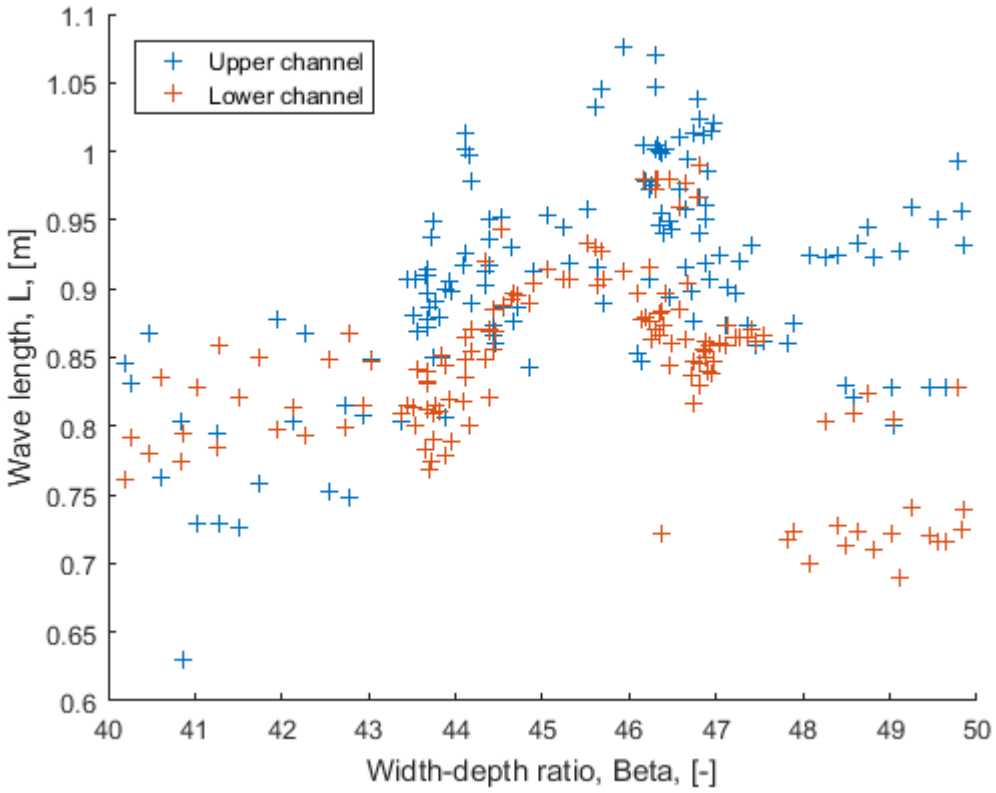

Figure 28 the along channel mean wavelength against the along channel mean width depth ratio for the upper and lower channel.

It was found that there is a positive linear relationship between the along channel mean wave of the bed and the width-depth ratio (β) of the estuary for the first 900 cycles (see Figure 27). These results are based on the DEM data. Although the trend in the DEM data and bluevalue data is comparable, as seen in Figure 20, the bluevalue data has too much variability on the short time scale. Instinctively, this relation is not expected. Since by increasing the width-depth ratio, the width is increased more than the depth. As a result, the width is increased more than the difference between the top of the bars and the depth of the channels, assuming that the bar height does not increase. A clear relationship between the bar-channel wavelength and width-depth ratio could not be found (see Figure 28). From the comparison between Figure 27 and Figure 28 it can be seen that the bar-channel wavelength shows more scatter compared to the amplitude. This can be explained by the larger variation through time of the bar-channel wavelength compared to the amplitude (see Figure 19 and Figure 20). Also there could not be found a relationship between the bar-channel wavelength and the averaged flow velocity over a tidal cycle or the water depth of the estuary (see Figure 29 and Figure 30). For both these parameters, it can be seen that the entire range could be found for every bar-channel wavelength.

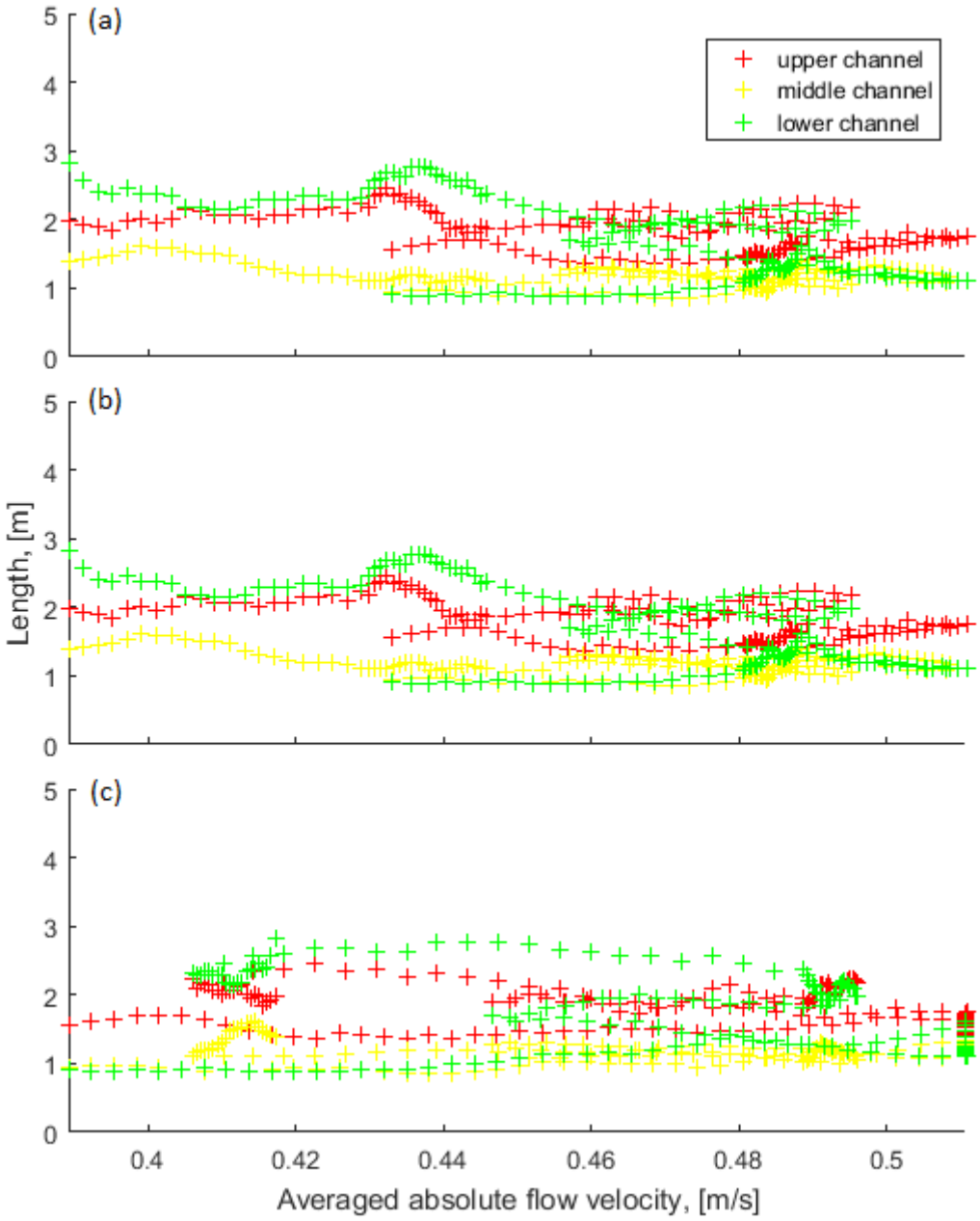

Figure 29 bar channel wavelength of the upper, middle and lower channel against the along channel, tidally averaged flow velocity for the total (a), right (b) and left (c) part of the system.

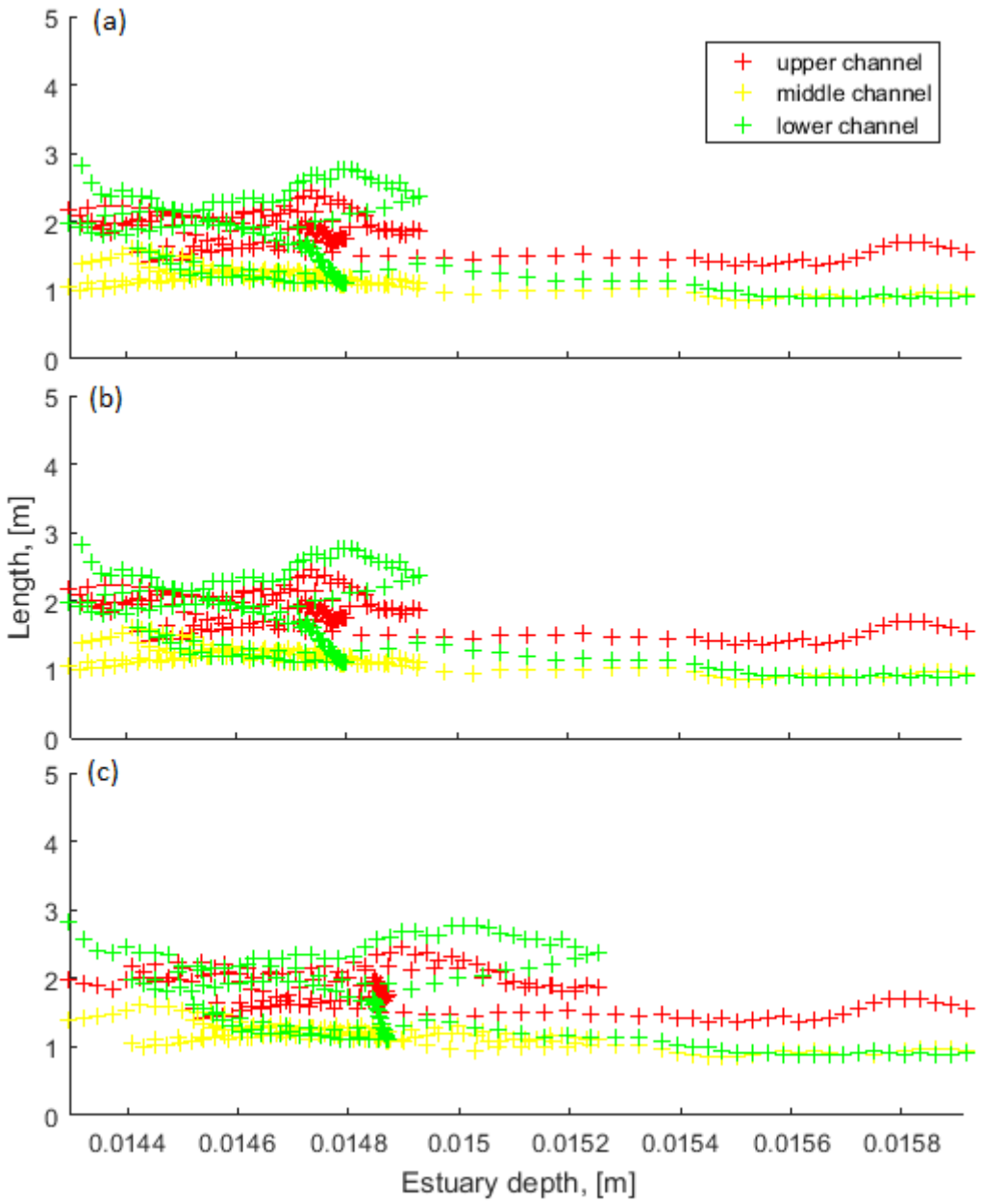

Figure 30 bar channel wavelength of the upper, middle and lower channel against the along channel averaged depth for the total (a), right (b) and left (c) part of the system.

4. Discussion

4.1 Bar-channel wave

4.1.1 Length

Bar channel wavelength can be predicted by the width of the estuary, as stated by Leuven et al. (2016), by multiplying the estuary width by two (see Figure 19). However, in both the left and the right side of the system there are two short periods of large growth, followed by a short period of large reduction in bar wave length. The growth is a result from the migration of the bars out of the seaward side of the channel, disrupting the prediction by Leuven et al. (2016). The decrease in bar-channel wavelength on the other hand can be explained by the formation of a new bar, filling up the new available space. The scaling of the bar length to the system width can also be found in rivers (Kleinhans and van den Berg, 2011) and in the sedimentary record (Dalrymple and Rhodes, 1995; Dalrymple and Choi, 2007).

Since there is still a slight growth of the estuary width it can be hypothesized that the bar-channel wavelength is not influenced by the width of the estuary, as state by Leuven at al. (2016) but rather that the estuary width is influenced by the bar-channel wavelength. The quick growth of the bar-channel wavelength cannot be matched by the growth of the estuary width, which is a more time consuming process (see Figure 19 and Figure 22). After the period of growth however, the predicted bar-channel wavelength becomes more comparable or slightly larger than the actual bar-channel wavelength. This is the period where the estuary width and bar-channel wavelength are in balance.

However, in literature it can also be found that the bar length in estuaries scale to tidal properties. The theory of Seminara and Tubino (2001) predicts the bar length to increase with increasing tidal amplitude and Schramkoski et al. (2002) are predicting that the bar length scales to the tidal excursion length. Also in river bar literature, some theories predict bar length on the basis of hydrologic parameters (Crosato and Mosselman, 2009), but it fails to predict the bar-channel wavelength (see Figure 31). On the assumption the main tidal properties are only influenced by the estuary water depth and the flow velocities, it can safely be sad that these relationships could not be found in this study.

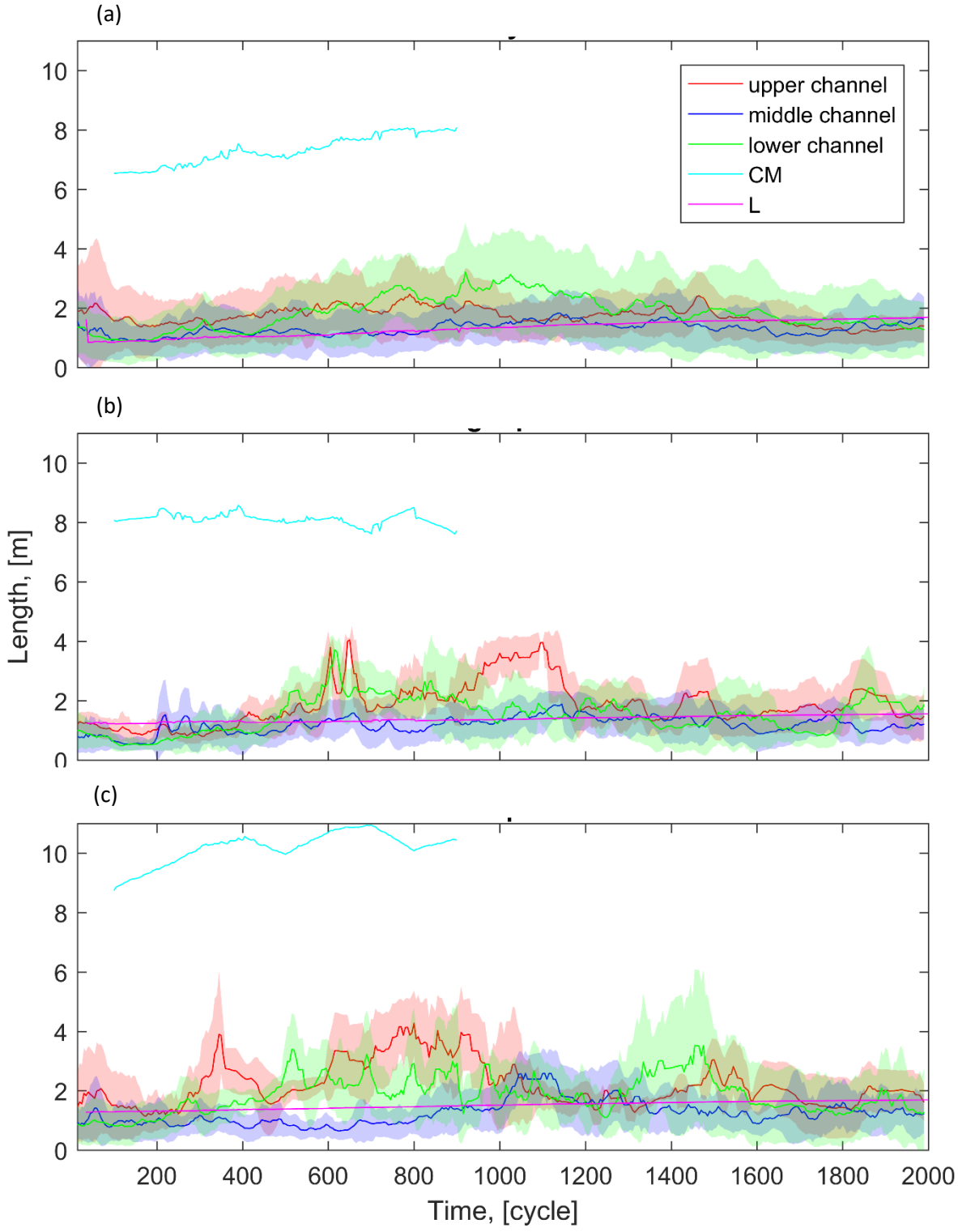

Figure 31 the along-channel mean of the bar-channel wavelength of the bed and associated standard deviation (shaded area) of the middle of the estuary, upper and lower channel through time of the entire system (a), right part (b) and left part (c) (Figure 15). The light blue (CM) and purple (L) are the predicted wave lengths using the method of Crosato and Mosselman (2009) and Leuven et al. (2016), respectively. Results are identical to Figure 19, however the prediction of Crosato and Mosselman (2009) is added.

However, sediment transport in estuaries is solely controlled by hydrodynamics and sediment properties as suggested by Billy et al. (2012). They found that the width and length of the bars in the Gironde estuary increase during long periods of high river discharge. This can be explained by the fact that during periods of high river discharge, the fluvial sediment input is larger while the sediment input in the experiment is more constant caused by the more constant widening of the estuary. This input of sediment increases the bar volume and with that, the bar length. Although this correlation is found and suggested, statistical it is not significant. Also van Leeuw and de Swart (2004) found that the bar length is related to the embayment width and hydrodynamic properties in a semi-enclosed embayment. In this model study, both the global and local patterns are modelled. The modelling of global patterns can cause changes in channel width. It was found that the local patterns, called tidal sand bars, are scaling to the embayment width. These tidal sand bars are mainly growing due to the divergence of the advective transport, which relates to the transport of the tide. Both these studies are suggesting that the tidal bar length depends on both the channel width and hydrodynamic properties.

Overall it can be concluded that the bar length or bar-channel wavelength is found to be related to the channel width based on empirical studies (Dalrymple and Rhodes, 1995; Dalrymple and Choi, 2007; Kleinhans and van den Berg, 2011; Leuven et al., 2016; this study) and to hydrodynamic properties based on model studies (Seminara and Tubino, 2001; Schramkoski et al., 2002; Crosato and Mosselman, 2009). Only Billy et al. (2012) and Leeuw and de Swart (2004) found some evidence that tidal bar length could be related to both the tidal property and estuary width. This can probably be explained by the fact that empirical studies do not fully understand the hydrodynamics of tides, while the model result fail to couple the hydrodynamics and sediment transport correctly.

4.1.2 Amplitude

In this research it is found that the amplitude of the bars only increases during the period of growth. This is indicated by the blue-values and the DEM measurement available. After this point there is a slight decrease in resulting in a more stable bar-channel wave amplitude. This growth in the first 1000 cycles and afterwards decrease can also be seen in the bar-channel wavelength, although the variability through time is larger. Another similarity with the bar-channel wavelength, is that the left part of the system develops roughly 200 cycles earlier than the right part. This is mostly visible in the ending time of the period of growth.

Unfortunately, there is only little literature available about bar-channel wave amplitude or bar height in estuary systems at this moment, however some river literature is available. The development during this experiment shows great similarity with the numerical model of Defina (2003). The main goal of this model was the difference in reaction on small initial bumps in the river bed. In this numerical model they also found that the bar amplitude first increases, from which there is a small decrease to get an equilibrium amplitude afterwards. Defina (2003) also found that, no matter the initial disturbance, the equilibrium bar-channel wavelength and amplitude are strictly related as is the celerity. In this research the development through time of the bar-channel wavelength and amplitude are also comparable indicating a similar relationship.

Tubino (1991) found in their flume experiment that the bar amplitude in river mainly grows during flood events, when water levels and flow velocities are high. It is also suggested by Villard and Church (2005) that bedforms, including bars, develop during stages of high flow. This increase in bar amplitude is mainly a consequence of sediment advection, which is related to the transport of the sediment by large dunes during high flows. However, in tidal environments the water level and flow velocities are not necessarily in phase. But to increase the height and thus the amplitude of the bar, water levels should be higher than the bar and flow velocities should be high enough to transport sediments.

Besides the dependence of the bar-channel wave amplitude to length, it also is found in this research that the bar-channel wave amplitude has a positive relationship to the width depth ratio (see Figure 27). However, this data is based on the DEM measurements, only available during the

first 900 cycles. This means that these results only capture the period of growth. This relation between the bar-channel wave amplitude and estuary width-depth ratio is also found by the numerical model of Colombini and Tubino (1991) and the flume experiment of Jang and Shimizu (2010), of which both are river based. In the model of Colombini and Tubino (1991) the width-depth ratio bar-channel wave amplitude relation is almost linear for all the calculated bar modes with weakly and fully non-linear equations until a width-depth ratio of 20. The experiment of Jang and Shimizu (2010) on the other hand show a continues positive relation for all the width depth ratios and experiments. However, the relation linearity in this experiment decreases by decreasing the critical submerged angle of response. This also decreases the bar amplitude for the same width-depth ratio, because of the decrease in possible steepness of the bars.

Although there is big absence on estuary bar-channel wave amplitude and bar height, it can be concluded that the results found in this study relate well to river bar-channel wave amplitude literature. It was found that the length and amplitude of a bar-channel wave relate well (Defina, 2003). In this study it was found that there is a relation between de bar-channel wave amplitude and the width to depth ratio as suggested by Colombini and Tubino (1991) and Jang and Shimizu (2010). Ultimately, also these dynamics could be related to the hydrodynamics (Tubino, 1991; Villard & Church, 2005).

4.2 Cross-sectional inner and outer bend location

It was found that the inner bends displayed a step like migration and the outer bends migrated at a more constant pace. This suggest that the outer bend is not influenced by the inner bend and so bar push theory does not hold in this experiment. If this was the case, the outer bend would display a similar step like behaviour as the inner bend or follow with some time lag. However, it not necessarily rejects or advocates for bank pull theory, because there is no clue whether the outer bend influences the inner bend or not. The step-like migration of the inner bend could result from the constant influence of the outer as the straw that broke the camel's back, triggering a sudden shift now and then. However, this difference in migration could also be used to advocate that the outer bend does not influence the inner bend, since otherwise a more similar migration could be expected.

Also on bend push or pull theories, the amount of estuary literature is minimal. However, Gabet (1998) monitored a tidal channel in a saltmarsh. The downside of this is that the scale is some magnitudes smaller than tidal estuary channels, making other mechanisms like roots and animals influence the bends. However, the upside is found in the fact that the sediment type is comparable to tidal estuary channels, the channels are affected by the reversal of flow and timespans of changes are smaller. The figures of Gabet (1998) do suggest that the main driver of cross-sectional location change of the bends is the bank pull theory. However, in this case both the inner and outer bend show a step like change in location. This is caused by the fact that, due to plant roots, erosion of the upper bank is slower than the lower bank. As a result, the bank is undercut and creating a slump block in the outer bend and with this changing the location of the outer bend in a short amount of time.

Eke et al. (2014) found that both push and pull theories can be true depending on the bank characteristics, with a river numerical model. Increasing the reference erosion, thus increasing the migration rate of the outer bend, pushes the system to bank pull. While increasing the reference deposition, thus increasing the migration rate to the inner bend, pushes the system more to bar push. However, he also identified that in time, the system always goes to a state of equal inner bank deposition and outer bank erosion without indication of bank pull or bar push. Van de Lageweg et al. (2014) on the other hand found with an experimental river set-up that bank pull is the driving force behind band migration. The erosion of the outer bend causes a widening of the flow, which results in a decrease in the flow velocities. This makes it possible for fine sediments to be deposited in the inner bend.

4.3 Limitations and further research

In this research the driving force for the morphological relations found could not be indicated. This can be explained by the fact that this research only conducted flow velocity measurements during the first 900 cycles with a time interval of 100 cycles. Firstly, this is only the time span of the periods of chaos and growth. There could not be found a relation between the flow velocity and bar-channel wavelength during this period. Secondly, the low frequency of the measurements is causing a very limited amount of data. For future research it is thus recommended to continuous measure the flow velocities with an automatic non-contact water monitoring device, like a doppler radar surface flow sensor.

During this research it became apparent that the knowledge of the relation between the hydrodynamics and morphodynamics of estuaries in literature is also lacking. However, most of the morphological features in estuaries could be related to their counterparts found in rivers. A possible comparison of the hydrodynamics of estuaries and rivers can be river floods. It is general known that most morphological changes happen during high discharges in rivers (Tubino, 1991; Ham and Church, 2000; Villard and Church, 2005). Tubino (1991) used unsteady flow parameters to predict bar-channel wave amplitude. Since tidal flows are also unsteady, a possible starting point in further understanding between the morphodynamics and hydrodynamics of an estuary can be converting river flood theories to a bidirectional flood theory suitable for tides. This can be done by subdividing the tidal cycle in different segments based on the absolute flow velocities. The larger flow velocity periods can be treated in a river flood theory as the floods and the low flow periods, which are not able to transport sediments, as non-flood stages. However, care must be taken that in rivers, water depth and flow velocity are mostly in phase, while this is not necessary the case for tidal flows. The knowledge found in this theoretical approach could later be applied to practical experiments.

5. Conclusion

In this research the behaviour estuarine bars and bends in a developing, initial straight channel, system was studied. For this purpose, tilting flume experimental data was analysed. The pre-dug channel in the flume was on both sides connected to a water reservoir, acting like a sea. This was done to increase the simplicity of the tidal signal by decreasing the asymmetric behaviour of it at the beginning of the experiment. It took 200 successive tidal cycles for a distinct alternation between channels and shoals developed, also visible in well-known natural estuaries like Western Scheldt (van Veen, 1950)

The analysed experiment shows the largest dynamics of the bars and bend location during the first 1200 cycles of the experiment, called the periods of chaos and growth. During the period of growth, the bars and bend are migrating away from the middle of the flume. This increases the bar channel wave length. Besides the length, also the amplitude of the bar channel wave is increased. After this period of high dynamics, the earlier named features show a small decrease and become more stable, the period of stabilization. Also the width of the estuary shows the fastest growth during the period of growth. Although smaller, the width is after this point still growing until the end of the analysis of the experiment.

It was found that the change of location of the outer bend was mostly larger than the inner bend. This results in the increase of the channel width in the bends. The other distinct behaviour of the cross-sectional location of the bends is the step wise change of the inner bend compared to the constant change of the outer bend. This indicates that the inner bend does not influence the outer bend, which does not follow this step wise migration with or without some time lag, thus indicating that bar push theory does not hold for these experimental results.

From this study it can be concluded that the main growth of the morphodynamic features of an estuary is primary during the beginning of existence, as expected. It is found that the dimensions of the bars do show a similar behaviour through time, although the short term dynamics of the bar-channel wavelength is higher compared to the amplitude. Also the longitudinal migration of the bends shows a similar periodicity. This periodicity is less well seen in the width of the estuary, which kept increasing, however slower, during the period of stabilization. The period of growth is ended slightly after the last DEM and flow velocity measurement. This has two implications: firstly, it could not be compared how the flow velocities changed from the period of growth to the period of stabilization and secondly, it could not be seen if the emptying of the flume in need of the DEM measurement did alter the experimental results.

It can be concluded that the dimensions, width and depth of the estuary are related and possible also the bends. This is of great importance for the knowledge about the natural systems, since it can be expected that human intervention of one part of the system, e.g. dredging, will cause a reaction of the rest of this system.

Acknowledgments

I want to thank both my supervisors, Dr Maarten Kleinhans and MSc Jasper Leuven, for their critical input, their patience that I pushed to the limits and for providing me with the critical data for this research. More than anyone, I would like to thank my parents who always supported me and provided me with wealth to study and follow my dream to be a cyclist.

References

Ahnert, F. (1960). Estuarine meanders in the Chesapeake Bay area. *Geographical review*, *50*(3), 390-401. DOI: 10.2307/212282

Barbier, E. B., Hacker, S. D., Kennedy, C., Koch, E. W., Stier, A. C., & Silliman, B. R. (2011). The value of estuarine and coastal ecosystem services. *Ecological monographs, 81*(2), 169-193. DOI: 10.1890/10-1510.1

Billy, J., Chaumillon, E., Féniès, H., & Poirier, C. (2012). Tidal and fluvial controls on the morphological evolution of a lobate estuarine tidal bar: The Plassac Tidal Bar in the Gironde Estuary (France). *Geomorphology, 169*, 86-97. DOI: 10.1016/j.geomorph.2012.04.015

Blanckaert, K., Kleinhans, M. G., McLelland, S. J., Uijttewaal, W. S., Murphy, B. J., Van de Kruijs, A., ... & Chen, Q. (2013). Flow separation at the inner (convex) and outer (concave) banks of constant-width and widening open-channel bends. *Earth Surface Processes and Landforms*, *38*(7), 696-716. DOI: 10.1002/esp.3324

Bolle, A., Wang, Z. B., Amos, C., & De Ronde, J. (2010). The influence of changes in tidal asymmetry on residual sediment transport in the Western Scheldt. *Continental Shelf Research*, *30*(8), 871-882. DOI: 10.1016/j.csr.2010.03.001

Colombini, M., & Tubino, M. (1991). Finite-amplitude free bars: a fully non-linear spectral solution. *Euromech, 262*, 163-169. Retrieved from https://www.researchgate.net/profile/Marco_Colombini2/publication/287879134_Finite_amplitude_free-bars_a_fully_nonlinear_spectral_solution/links/56b36b9b08ae75a092d00c87.pdf

Crosato, A., & Mosselman, E. (2009). Simple physics-based predictor for the number of river bars and the transition between meandering and braiding. *Water Resources Research*, *45*(3). DOI: 10.1029/2008WR007242

Dalrymple, R. W., & Choi, K. (2007). Morphologic and facies trends through the fluvial–marine transition in tide-dominated depositional systems: a schematic framework for environmental and sequence-stratigraphic interpretation. *Earth-Science Reviews, 81*(3-4), 135-174. DOI: 10.1016/j.earscirev.2006.10.002

Dalrymple, R. W., & Rhodes, R. N. (1995). Estuarine dunes and bars. *Developments in sedimentology*, 53, 359-422. DOI: 10.1016/S0070-4571(05)80033-0

Dalrymple, R. W., Zaitlin, B. A. & Boyd, R. (1992). Estuarine facies models: conceptual basis and stratigraphic implications. *Journal of Sedimentary Petrology, 62*(6), 1130-1146. DOI: 10.1306/D4267A69-2B26-11D7-8648000102C1865D

Defina, A. (2003). Numerical experiments on bar growth. *Water Resources Research, 39(*4), 1092. DOI: 0.1029/2002WR001455

Eke, E., Parker, G., & Shimizu, Y. (2014). Numerical modeling of erosional and depositional bank processes in migrating river bends with self-formed width: Morphodynamics of bar push and bank pull. *Journal of Geophysical Research: Earth Surface, 119*(7), 1455-1483. DOI: 10.1002/2013JF003020

Escoffier, F. F. (1977). Hydraulics and Stability of Tidal Inlets.

Fischer, H.B. (1979). Mixing and dispersion in estuaries. *Annual review of fluid mechanics, 8*(1): 107-133. DOI: 10.1146/annurev.fl.08.010176.000543

Gabet, E. J. (1998). Lateral migration and bank erosion in a saltmarsh tidal channel in San Francisco Bay, California. *Estuaries, 21*(4), 745-753. DOI: 10.2307/1353278

Garotta, V., Rummel, A. C., & Seminara, G. (2008). Long-term morphodynamics and hydrodynamics of tidal meandering channels. Paper presented at the River, Coastal and Estuarine Morphodynamics conference, Taylor and Francis/Balkema, Enschede, (pp. 163-168). Retrieved from http://www.dicat.unige.it/flubio/fellowspapers/A037_RCEM07.pdf

Ham, D. G., & Church, M. (2000). Bed-material transport estimated from channel morphodynamics: Chilliwack River, British Columbia. *Earth Surface Processes and Landforms: The Journal of*

the British Geomorphological Research Group, 25(10), 1123-1142. DOI: 10.1002/1096-9837(200009)25:10<1123::AID-ESP122>3.0.CO;2-9

Hibma, A., Stive, M. J. F., & Wang, Z. B. (2004). Estuarine morphodynamics. *Coastal Engineering*, *51*(8-9), 765-778. DOI: 10.1016/j.coastaleng.2004.07.008

Hibma, A., De Vriend, H. J., & Stive, M. J. F. (2003). Numerical modelling of shoal pattern formation in well-mixed elongated estuaries. *Estuarine, Coastal and Shelf Science*, *57*(5-6), 981-991. DOI: 10.1016/S0272-7714(03)00004-0

Hoitink, A. J. F., Wang, Z. B., Vermeulen, B., Huismans, Y., & Kästner, K. (2017). Tidal controls on river delta morphology. *Nature geoscience*, *10*(9), 637–645. DOI: 10.1038/NGEO3000

Jang, C. L., & Shimizu, Y. (2005). Numerical simulations of the behavior of alternate bars with different bank strengths. *Journal of Hydraulic Research*, *43*(6), 596-612. DOI: 10.1080/00221680509500380

Jay, D.A., & Musiak, J.D. (1994). Particle trapping in estuarine tidal flows. *Journal of Geophysical Research: Oceans, 99*(C10), 20445-20461. DOI:10.1029/94JC00971

Jeuken, M.C.J.L. Wang, Z.B. (2010). Impact of dredging and dumping on the stability of ebb–flood channel systems. *Coastal Engineering, 57*(6), 553-566. DOI: 10.1016/j.coastaleng.2009.12.004

Kleinhans, M. G., Leuven, J. R., Braat, L., & Baar, A. (2017a). Scour holes and ripples occur below the hydraulic smooth to rough transition of movable beds. *Sedimentology*, *64*(5), 1381-1401. 10.1111/sed.12358

Kleinhans, M. G., Schuurman, F., Bakx, W., & Markies, H. (2009). Meandering channel dynamics in highly cohesive sediment on an intertidal mud flat in the Westerschelde estuary, the Netherlands. *Geomorphology*, *105*(3-4), 261-276. DOI: 10.1016/j.geomorph.2008.10.005

Kleinhans, M. G., & van den Berg, J. H. (2011). River channel and bar patterns explained and predicted by an empirical and a physics-based method. *Earth Surface Processes and Landforms, 36*(6), 721-738. DOI: 10.1002/esp.2090

Kleinhans, M. G., Van Der Vegt, M., Leuven, J., Braat, L., Markies, H., Simmelink, A., & Van Maarseveen, M. (2017b). Turning the tide: comparison of tidal flow by periodic sea level fluctuation and by periodic bed tilting in scaled landscape experiments of estuaries. Earth Surface Dynamics, 5(4), 731-756. Retrieved from https://dspace.library.uu.nl/bitstream/handle/1874/361728/Turning.pdf?sequence=1&isAllowed=y

Kleinhans, M. G., Van der Vegt, M., Van Scheltinga, R. T., Baar, A. W., & Markies, H. (2012). Turning the tide: experimental creation of tidal channel networks and ebb deltas. *Netherlands Journal of Geosciences*, *91*(3), 311-323.

Kleinhans, M. G., Van Scheltinga, R. T., Van Der Vegt, M., & Markies, H. (2015). Turning the tide: growth and dynamics of a tidal basin and inlet in experiments. *Journal of Geophysical Research: Earth Surface*, *120*(1), 95-119. DOI: 10.1017/S0016774600000469

Leuven, J. R., Braat, L., van Dijk, W. M., de Haas, T., Onselen, E. V., Ruessink, B. G., & Kleinhans, M. G. (2018). Growing forced bars determine non-ideal estuary planform. *Journal of Geophysical Research: Earth Surface.* DOI: 10.1029/2018JF004718

Leuven, J. R. F. W., Kleinhans, M. G., Weisscher, S. A. H., & Van der Vegt, M. (2016). Tidal sand bar dimensions and shapes in estuaries. *Earth-Science Reviews*, *161*, 204-223. DOI: 10.1016/j.earscirev.2016.08.004

MacCready, P., & W.R. Geyer. (2010) Advances in estuarine physics. *Annual Review of Marine Science,* (2), 35-58. DOI: 10.1146/annurev-marine-120308-081015

Marra, W. A., Parsons, D. R., Kleinhans, M. G., Keevil, G. M., & Thomas, R. E. (2014). Near-bed and surface flow division patterns in experimental river bifurcations. *Water Resources Research*, *50*(2), 1506-1530. DOI: 10.1002/2013WR014215

Nguyen, A. D. 2008. Salt Intrusion, Tides and Mixing in Multi-Channel Estuaries (Doctoral dissertation). Retrieved from https://www.taylorfrancis.com/books/9781439828342

Pritchard, D. W. (1967). What is an estuary: physical viewpoint. *American Association for the Advancement of Science, 83*, 3-5. Retrieved from: http://hdl.handle.net/1969.3/24383

Reynolds, O. (1889, 1890, 1891). *First, second and third report of the committee appointed to investigate the action of waves and currents on the beds and foreshores of estuaries by means of working models.* Reprinted in: Papers on mechanical and physical subjects, Technical report I, II and III: British Association Report.

Savenije, H.H.G. 1993. Predictive model for salt intrusion in estuaries. *Journal of Hydrology*, *148*(1-4), 203-218. DOI:10.1016/0022-1694(93)90260-G

Schramkowski, G. P., Schuttelaars, H. M., & De Swart, H. E. (2002). The effect of geometry and bottom friction on local bed forms in a tidal embayment. *Continental Shelf Research*, *22*(11-13), 1821-1833. DOI: 10.1016/S0278-4343(02)00040-7

Seminara, G., & Tubino, M. (2001). Sand bars in tidal channels. Part 1. Free bars. *Journal of Fluid Mechanics*, *440*, 49-74. DOI: 10.1017/S0022112001004748

Simpson, J. H., Williams, E., Brasseur, L. H., & Brubaker, J. M. (2005). The impact of tidal straining on the cycle of turbulence in a partially stratified estuary. *Continental Shelf Research*, *25*(1), 51-64. DOI: 10.1016/j.csr.2004.08.003

Stefanon, L., Carniello, L., D'Alpaos, A., & Lanzoni, S. (2010). Experimental analysis of tidal network growth and development. *Continental Shelf Research*, *30*(8), 950-962. DOI: 10.1016/j.csr.2009.08.018

Stokes, G.G. 1847. On the theory of oscillatory waves. *Transactions of the Cambridge Philosophical Society*, *8,* 441–455.

Swinkels, C.M., Jeuken, C.M.C.J.L., Wang, Z.B., Nicholls, R.J. (2009). Presence of connecting channels in the Western Scheldt estuary. *Journal of Coastal Research 25*(3), 627–640. DOI: 10.2112/06-0719.1

Tambroni, N., Bolla Pittaluga, M., & Seminara, G. (2005). Laboratory observations of the morphodynamic evolution of tidal channels and tidal inlets. *Journal of Geophysical Research: Earth Surface*, *110*(F4). DOI: 10.1029/2004JF000243.

Tubino, M. (1991). Growth of alternate bars in unsteady flow. *Water Resources Research, 27*(1), 37-52. DOI: 10.1029/90WR01699

Van de Lageweg, W. I., van Dijk, W. M., Baar, A. W., Rutten, J., & Kleinhans, M. G. (2014). Bank pull or bar push: What drives scroll-bar formation in meandering rivers? *Geology, 42*(4), 319-322. DOI: 10.1130/G35192.1

Van Leeuwen, S. M., & De Swart, H. E. (2004). Effect of advective and diffusive sediment transport on the formation of local and global bottom patterns in tidal embayments. *Ocean Dynamics, 54*(3-4), 441-451. DOI: 10.1007/s10236-004-0092-9

Van Veen, J. (1950). Ebb and flood channel systems in the Netherlands tidal waters, reprint of the original text. *Journal of the Royal Dutch Geographical Society, 67*, 303-325.

Villard, P. V., & Church, M. (2005). Bar and dune development during a freshet: Fraser river estuary, British Columbia, Canada. *Sedimentology, 52*(4), 737-756. DOI: 10.1111/j.1365-3091.2005.00721.x

Vlaswinkel, B. M., & Cantelli, A. (2011). Geometric characteristics and evolution of a tidal channel network in experimental setting. *Earth Surface Processes and Landforms*, *36*(6), 739-752. DOI: 10.1002/esp.2099

Zhang, W., Feng H., Zheng J., Hoitink A.J.F., Van Der Vegt M., Zhu Y., & Cai H. (2013). Numerical simulation and analysis of saltwater intrusion lengths in the pearl River Delta, China. *Journal of Coastal Research, 29*(2), 372-382. DOI: 10.2112/JCOASTRES-D-12-00068.1

Appendix 1: List of figures